Inorganic Chemistry

pubs.acs.org/IC

Article

The Reactivity of Phosphanylphosphinidene Complexes of Transition Metals Toward Terminal Dihaloalkanes

Anna Ordyszewska, Natalia Szynkiewicz, Jarosław Chojnacki, Jerzy Pikies, and Rafał Grubba*

Cite This: *Inorg. Chem.* 2020, 59, 5463−5474

Read Online

ACCESS | Metrics & More | Article Recommendations | Supporting Information

ABSTRACT: The reactivities of phosphanylphosphinidene complexes $[(DippN)_2W(Cl)(\eta^2\text{-}P{-}PtBu_2)]^-$ (**1**), $[(pTol_3P)_2Pt(\eta^2\text{-}P{=}PtBu_2)]$ (**2**), and $[(dppe)Pt(\eta^2\text{-}P{=}PtBu_2)]$ (**3**) toward dihaloalkanes and methyl iodide were investigated. The reactions of the anionic tungsten complex (**1**) with stochiometric $Br(CH_2)_nBr$ (n = 3, 4, 6) led to the formation of neutral complexes with a $tBu_2PP(CH_2)_3Br$ ligand or neutral dinuclear complexes with unusual tetradentate $tBu_2PP(CH_2)_nPPtBu_2$ ligands (n = 4, 6). The methylation of platinum complexes **2** and **3** with MeI yielded neutral or cationic complexes bearing side-on coordinated $tBu_2P{-}P$-Me moieties. The reaction of **2** with $I(CH_2)_2I$ gave a platinum complex with a $tBu_2P{-}P{-}I$ ligand. When the same dihaloalkane was reacted with **3**, the P—P bond in the phosphanylphosphinidene ligand was cleaved to yield tBu_2PI, phosphorus polymers, $[(dppe)PtI_2]$ and C_2H_4. Furthermore, the reaction of **3** with $Br(CH_2)_2Br$ yielded dinuclear complex bearing a tetraphosphorus $tBu_2PPPPtBu_2$ ligand in the coordination sphere of the platinum. The molecular structures of the isolated products were established in the solid state and in solution by single-crystal X-ray diffraction and NMR spectroscopy. DFT studies indicated that the polyphosphorus ligands in the obtained complexes possess structures similar to free phosphenium cations $tBu_2P^+{=}P{-}R$ (R = Me, I) or $(tBu_2P^+{=}P)_2$.

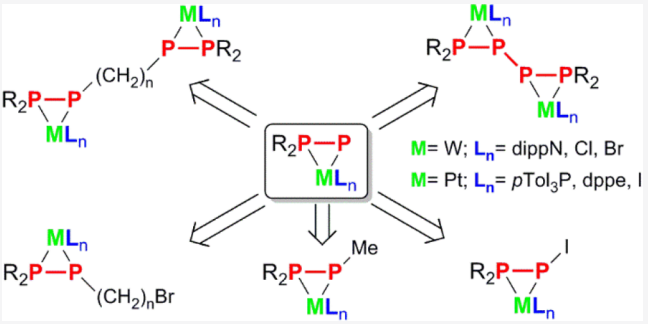

1. INTRODUCTION

The properties of phosphido and phosphinidene complexes of transition metals (TM) as synthetic tools in organic and inorganic chemistry have recently been intensely studied.[1] Formally, phosphinidene complexes can be divided into two classes: electrophilic, which are often very reactive transient species[2−6] except for the stable phosphinidene complexes of cobalt and vanadium described by Carty group,[7,8] and nucleophilic, which are generally isolable.[5,6,9] It is commonly accepted that the electrophilicity versus nucleophilicity of a phosphinidene complex is primarily determined by the electronic properties of the spectator ligands[10]—acceptor ligands (especially CO) that result in electrophilic complexes, whereas donor spectator ligands, such as NR and PR_3, result in nucleophilic complexes. From this point of view, phosphanylphosphinidene complexes, which we discuss in this paper ($[(DippN)_2W(Cl)(\eta^2\text{-}P{-}PtBu_2)]^-$ (**1**),[11] $[(pTol_3P)_2Pt(\eta^2\text{-}P{=}PtBu_2)]$ (**2**),[12] and $[(dppe)Pt(\eta^2\text{-}P{=}PtBu_2)]$ (**3**)[13]) must be considered nucleophilic species (Scheme 1). Similar nucleophilic phosphanylphosphinidene complexes $[(\eta^2\text{-}R_2PP)Nb\{N(Np)(3,5\text{-}Me_2\text{-}C_6H_3)\}_3]$ and $[(\eta^2\text{-}R_2PP)W\{N(iPr)(3,5\text{-}Me_2\text{-}C_6H_3)\}_3]^+$ were studied by Cummins group.[14,15]

The nucleophilicity of these species can also be enhanced by a donor phosphanyl group ($PtBu_2$) in the phosphinidene ligand. It should be stressed that stable phosphanylphosphinidene $R_2P{=}P$ (R = nitrogen-based very bulky group) is singlet and electrophilic.[16] Reactivity studies on $tBu_2P{-}P{=}PtBu_2(Me)$[17] and DFT-calculations[18] revealed that transient $tBu_2P{-}P$ is also electrophilic. The nucleophilic phosphinidene complexes of early TM have been intensely studied and explored as P−R transfer vehicles to organic or inorganic molecules (phospha-Wittig reactivity). The first report concerned reactions of $[(N_3N)Ta^V{=}PR]$, N_3N = $(Me_3SiNCH_2CH_2)_3N$ (κ^3-*N*-chelating ligand) with aldehydes

Scheme 1. Phosphanylphosphinidene Complexes of W and Pt Used for Reactivity Studies

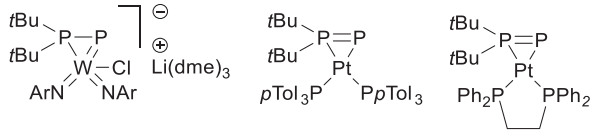

Received: January 10, 2020
Published: March 27, 2020

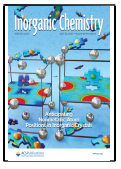

Scheme 2. Reactions of 1 with Dihaloalkanes

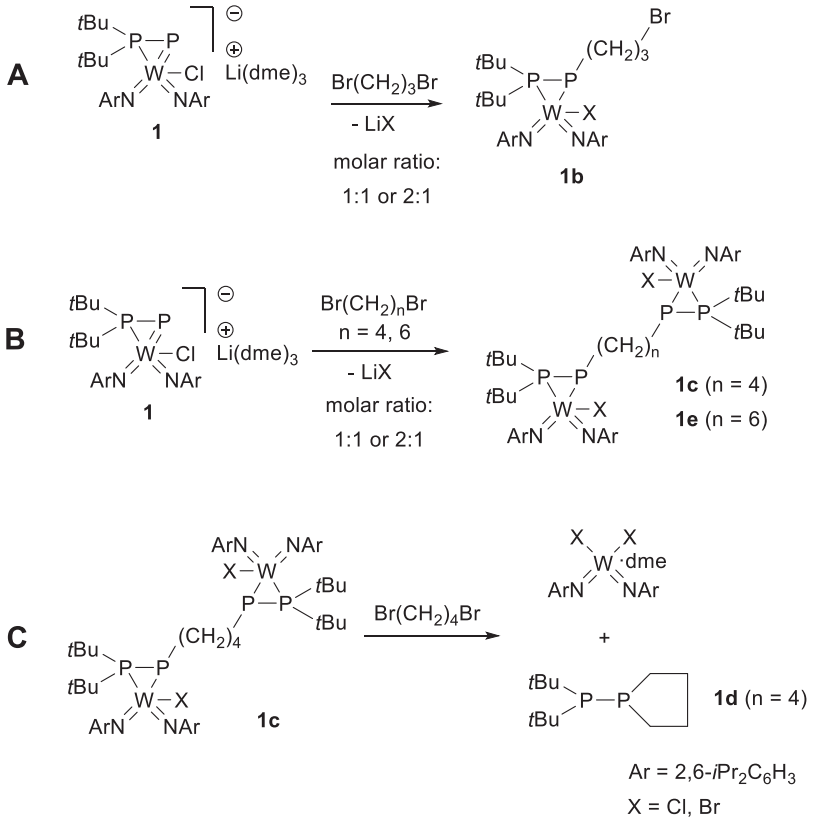

yielding the corresponding phosphenes.[19] Phosphinidene ate complex [(PNP)Sc^{III}(=PDmp)·LiBr] can transfer its P-Dmp moiety even to a Cp_2Zr-center, resulting in [Cp_2Zr^{IV}(=PDmp)(PMe_3)]. However, the analogous phosphinidene transfer was not observed for the reaction involving a Cp_2Ti-center.[20] Similarly, zirconium complexes [$Cp^*_2Zr(PPh)_2$] and [$Cp^*_2Zr(PPh)_3$] do not display phospha-Wittig reactivity.[21] Otherwise, [Cp_2Zr^{IV}(=PDmp)(PMe_3)] itself displayed high reactivity toward electrophilic reagents.[22] Similarly, [Cp_2Zr^{IV}(=PMes*)(PMe_3)] showed high phospha-Wittig reactivity and converted aldehydes and ketones into phosphenes. It reacted with CH_2Cl_2 and $CHCl_3$ yielding the related phosphenes as well.[23] Recently, the high reactivity of the phosphido complex [^{Me}NacNacTi^{III}(Cl)(η^2-(Me_3Si)P—PR_2)] R_2 = tBu_2 or tBu(Ph) toward acetone, yielding Wittig products R_2P—P=$C(CH_3)_2$ was established.[24] The reactivity of nucleophilic phosphinidene complexes of iron, iridium, and platinum toward electrophilic reagents was briefly studied. Dinuclear complexes [Fe_2(η-PR)(η-CO)$(CO)_2$] (R = *c*Hex or Ph) reacted with MeI, yielding related [Fe_2{η-P(Me)R}(η-CO)$(CO)_2$]I[25,26] and forming new P—C bonds. The reaction of iridium complex [Cp*(PPh_3)(=PMes*)] with CH_2I_2 or CHI_3 yielded the related phosphenes.[27] The reaction of dinuclear Pt^0 complex [Pt(dppe)(μ-PMes)]$_2$ with MeI afforded [Pt(dppe){μ-P(Me)Mes}]$_2^{2+}$, which is classically nucleophilic and undergoes protonation, oxidation, and Lewis acid complexation.[28] In comparison to phosphinidene TM complexes, the phosphinidene complexes of main group elements are significantly less explored. Since the introduction of stable carbenes, they found a wide application to stabilize low valent compounds of main group elements including phosphinidene group.[29−32]

The syntheses and properties of phosphanylphosphinidene complexes of TM are one of the main research interests of our group. We have elaborated practical methods for accessing a variety of complexes with R_2P—P ligands using R_2P—P($SiMe_3$)Li[11,12,33−36] or using tBu_2P—P=PtBu_2(X) (X = Me or Br)[17] as transport vehicles for the tBu_2P—P moiety. The reactivity of anionic W^{VI} complex [(DippN)$_2$(Cl)W(η^2-tBu_2P—P)]$^-$ was studied in more detail.[11] It was nucleophilic and reacted with electrophilic reagents, such as Ph_2PBr, $PhPCl_2$, or MeI, forming new P—P or P—C bonds.[34,35] However, the nucleophilicity of this complex is rather low. It yields adducts with Lewis acids such as MCl_3 (M = Al or Ga) or $Cr(CO)_5$·THF, but these reactions are clearly reversible.[18] Chronologically, the first complexes reported with phosphanylphosphinidene ligands were [(R_3P)Pt^0(η^2-tBu_2P=P)].[37] They are strongly nucleophilic and differ significantly from phosphanylphosphinidene early TM complexes but their properties remain almost unexplored.[25] Herein, we report the reactions of [(DippN)$_2$W(Cl)(η^2-P—PtBu_2)]$^-$ (**1**), [($pTol_3$P)$_2$Pt(η^2-P=PtBu_2)] (**2**), and [(dppe)Pt(η^2-P=PtBu_2)] (**3**) with electrophilic dihaloalkanes X(CH_2)$_n$X (*n* = 2−6, X = Br, I) to investigate the effect of carbon chain length on the products as well as advance the field of phosphanylphosphinidene chemistry.

2. RESULTS AND DISCUSSION

The reactivity of phosphanylphosphinidene complex **1** toward dihaloalkanes was investigated (Scheme 2). The reaction of **1** with Br(CH_2)$_3$Br in a 1:1 molar ratio in DME is very clean and gave only tungsten complexes with tBu_2P—P(CH_2)$_3$Br (**1b**) as the ligand and LiX (X = Cl, Br) as main products (Scheme 2A). The $^{31}P\{^1H\}$ NMR spectrum of the reaction mixture

https://dx.doi.org/10.1021/acs.inorgchem.0c00091
Inorg. Chem. 2020, 59, 5463−5474

consists of only two pairs of doublets at 40.0/−125.3 ppm and at 36.9/−132.2 ppm, which can be attributed to complexes **1b-Cl** and **1b-Br**, respectively. These complexes differ only in the presence of chlorido (**1b-Cl**) or bromido ligands (**1b-Br**) directly bound to the tungsten atom. Moreover, the $^{1}J_{PP}$ coupling constants, with values of 375 Hz (**1b-Cl**) and 381 Hz (**1b-Br**), indicate that the P—P bond is retained in the newly formed ligand. Furthermore, the signals of **1b-Cl** and **1b-Br** in $^{31}P\{^{1}H\}$ NMR spectra are accompanied by $^{1}J_{PW}$ satellites ($^{1}J_{P1W}$ = 80 Hz), which confirm that the phosphorus ligand did not leave the coordination sphere of tungsten.

A comparison of the $^{31}P\{^{1}H\}$ NMR data of **1b-Cl/Br** with the NMR data of parent compound **1** reveals that the doublets attributed to the $P(CH_2)_3Br$ group in **1b-Cl/Br** are strongly upfield shifted compared to those in **1** (−125.3/−132.2 ppm vs 17.7 ppm). Moreover, in the $^{31}P\{^{1}H\}$ NMR spectra of **1b-Cl/Br** these doublets split into doublets of triplets ($^{2}J_{PH}$ = 12 Hz). On the other hand, the $^{31}P\{^{1}H\}$ NMR data of **1b-Cl/Br** are similar to those observed for $[(DippN)_2W(X)(1,2\text{-}\eta\text{-}tBu_2P{-}PCH_3)]$ (X= Cl, I) (**1a**) (44.1/−142.3 ppm and 33.7/−161.2 ppm, for the chloro- and iodo-derivatives, respectively), which were obtained previously by us.[35] Crystallization from a pentane solution gave yellow crystals in 48% yield, and the crystals contained **1b-Cl** and **1b-Br** in a 0.4:0.6 molar ratio according to the integrals of the ^{31}P NMR signals. According to X-ray analysis the crystals were a solid solution of **1b-Cl** and **1b-Br** occupying the same positions (a kind of static disorder). Furthermore, we reacted **1** with 1,2-dibromoethane in a 1:1 molar ratio in DME, which led to a mixture of polyphosphorus compounds according to $^{31}P\{^{1}H\}$ NMR analysis of the reaction solution. The only isolated product was $[(ArN)_2WX_2(dme)]$ (X = Cl, Br),[38] and its structure was confirmed both by NMR spectroscopy and X-ray analysis. Therefore, we assume that the $tBu_2P{-}P$ ligand leaves the coordination sphere of tungsten during this reaction.

The reactivity of **1** toward dihaloalkanes with longer aliphatic chains was also investigated. The progress of the reactions of **1** with $Br(CH_2)_nBr$ (n = 4, 6) in a 1:1 molar ratio was monitored spectroscopically and revealed the formation of products with $^{31}P\{^{1}H\}$ NMR spectra very similar to those of **1b-Cl/Br** (see Table 1).

Table 1. $^{31}P\{^{1}H\}$ NMR Data of Complexes 1b, 1c, and 1e

	chemical shift [ppm]		coupling constant [Hz]		
compound	(R-)P1	tBu_2P2	$^{1}J_{P1P2}$	$^{1}J_{P1W}$	$^{1}J_{P2W}$
1b-Cl	−125.3	40.0	375	80	17
1b-Br	−132.2	36.9	381	80	17
1c-Cl	−122.2	40.3	378	76	17
1c-Br	−129.1	37.2	383	80	17
1e-Cl	−122.1	40.5	378	80	18
1e-Br	−129.0	37.4	382	80	18

A cursory analysis of the $^{31}P\{^{1}H\}$ NMR spectra of the reaction mixtures would suggest the formation of a series of complexes analogous to **1b-Cl/Br**. However, isolation of the products of these reactions in the crystalline form and X-ray structural analysis revealed the formation of dinuclear complexes (**1c-Cl/Br**, **1e-Cl/Br**) with unusual tetradentate $tBu_2P{-}P(CH_2)_nP{-}PtBu_2$ ligands (Scheme 2B). As a result of halide exchange, these compounds were isolated as mixtures of isostructural chlorido and bromido complexes at a molar ratio of 1.3:0.7 according to the integrals of the ^{31}P NMR signals. The bromido complexes can be easily converted into the corresponding chlorido complexes by the addition of three-fold excess of anhydrous LiCl in DME (Figure S17). In the case of the reaction involving 1,4-dibromobutane, the composition of the reaction mixture changes over time. The $^{31}P\{^{1}H\}$ NMR spectrum of the reaction mixture after 0.5 h consists of only two sets of doublets, which can be attributed to **1c-Cl** and **1c-Br**. After prolonged stirring at room temperature, new resonances for **1d** appeared (δ 42.3 ppm (d, tBu_2P); −37.3 (d, **P** $(CH_2)_4$); $^{1}J_{PP}$ = 203 Hz), and this was accompanied by a decrease in the intensities of the signals of **1c-Cl/Br**. After 3 days, a high conversion of **1c-Cl/Br** into **1d** was observed. Furthermore, from this reaction mixture a significant amount of crystals of $[(ArN)_2WX_2(dme)]$ (X = Cl, Br) was isolated. In the first stage of this reaction, dinuclear complexes **1c-Cl/Br** are likely formed (Scheme 2C, n = 4). Next, **1c-Cl/Br** reacts with the remaining $Br(CH_2)_4Br$, yielding diphosphane **1d** consisting of a phospholane group and $[(ArN)_2WX_2(dme)]$ (X = Cl, Br) (Scheme 2C). This type of reactivity is reminiscent of the reaction of nucleophilic phosphinidene zirconium complex $[Cp_2Zr{=}PMes^*(PMe_3)]$ with 1,2-dichloroxylene, which led to the formation of phospholane $C_6H_4(CH_2)_2PMes^*$.[23] We did not observe the formation of the analogous diphosphanes with cyclic substituents from the reaction of equimolar amounts of **1** with $Br(CH_2)_nBr$ (n = 3, 6). We suspect that the formation of **1d**, containing a five-member phospholane ring, is thermodynamically favored. To verify this hypothesis, we calculated the ΔG° value for simplified ring-closing reactions: $tBu_2P{-}P(H)(CH_2)_nBr \rightarrow tBu_2P{-}P(CH_2)_n + HBr$ (n = 3−6) (see the SI for details). Indeed, the lowest and only negative value of ΔG° was found for reaction yielding **1d**. Notably, reactions with a 2-fold excess of **1** relative to $Br(CH_2)_nBr$ (n = 4, 6) gave the same dinuclear tungsten complexes as reactions with equimolar amounts of the substrates. Interestingly, the reaction of 1,3-dibromopropane even with excess **1** did not lead to a complex with $tBu_2P{-}P(CH_2)_3P{-}PtBu_2$ ligand. The space-filling model of **1c-Cl/Br**, which contains four carbon atoms in the aliphatic chain linking the two $P{-}PtBu_2$ groups (Figure S2), reveals that this complex is very crowded. Therefore, the formation of analogous complexes with less than four carbon atoms in the aliphatic chain is not favored because of the steric effects of the bulky imido ligands.

The isolation of complexes **1b**, **1c**, and **1e** in the crystalline form allowed us to discuss their solid-state structures in detail. The X-ray structures of **1b** and **1c** are presented in Figures 1 and 2, whereas the molecular structure of **1e** is depicted in Figure S1. Complex **1b** differs from complexes **1c** and **1e** in the number of metal centers and in the structure of the phosphorus ligands. In the solid-state structure of **1b**, both phosphorus atoms of the $tBu_2P{-}P(CH_2)_3Br$ ligand coordinate to the tungsten atom. Unlike **1b**, where the propane chain is terminated by a bromine atom, in compounds **1c** and **1e** the aliphatic chain is terminated by a second $tBu_2P{-}P$ group. The tetradentate $tBu_2P{-}P(CH_2)_nP{-}PtBu_2$ (n = 4, 6) ligands in **1c** and **1e** are side-on coordinated to two tungsten centers. Despite these differences, complexes **1b**, **1c**, and **1e** exhibit many structural similarities. All the mentioned complexes feature pentacoordinated tungsten atoms. Furthermore, the P1—P2, P1—W1, and P2—W1 distances are very similar with values in ranges of 2.150(4)−2.168(2) Å, 2.506(1)−2.516(2) Å, and 2.540(2)−2.583(2) Å, respectively. The P1—P2 bonds in **1b**, **1c**, and **1e** are longer than the corresponding distance in

https://dx.doi.org/10.1021/acs.inorgchem.0c00091
Inorg. Chem. 2020, 59, 5463−5474

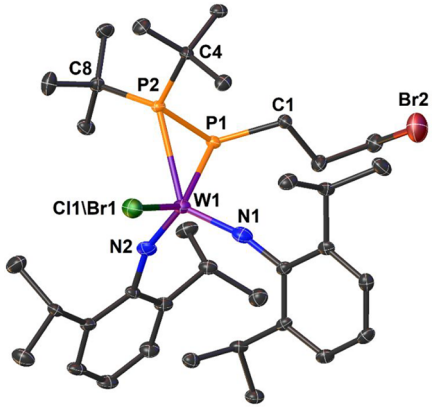

Figure 1. Molecular structure of complex **1b**. Displacement ellipsoids are shown at 50% probability. H atoms are omitted for clarity. Selected bond lengths (Å) and angles (°): P1—W1 2.508(2), P2—W1 2.583(2), P1—P2 2.155(2), C1—P1 1.869(4), ΣP1 291.9, ΣP2 338.5 (neglecting the P2—W1 bond), C1—P1—P2 113.4(2), C1—P1—P2—C4 7.8(3).

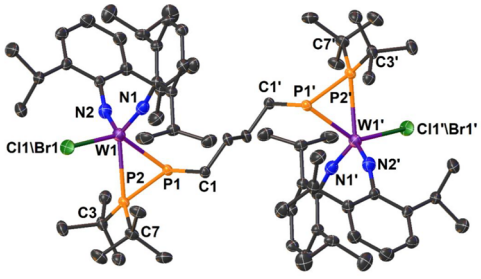

Figure 2. Molecular structure of complex **1c**. Ellipsoids are shown at 50% probability. H atoms are omitted for clarity. Selected bond lengths (Å) and angles (°): P1—W1 2.506(1), P2—W1 2.580(2), P1—P2 2.168(2), C1—P1 1.874(5), ΣP1 284.6, ΣP2 340.4 (neglecting the P2—W1 bond), C1—P1—P2 110.3(2), C1—P1—P2—C7 12.8(3). Atoms labeled with primes are related by symmetry code (1-x, 1-y, 1-z), i.e., symmetry center.

parent compound **1** (2.106(2) Å); however, they are still shorter than the sum of the single-bond covalent radii for P atoms (2.22 Å).[39] Furthermore, the P1—W1 bond distances in **1b, 1c**, and **1e** are significantly longer than that in **1** (2.406(1) Å), whereas the P2—W2 bond lengths are comparable to that observed in phosphanylphosphinidene complex **1** (2.571(1) Å). In comparison to **1b, 1c**, and **1e**, tungsten complexes possessing RP−PR′R″ ligand and PPW metallocycle such as $[Cp(CO)_2W\{P(tBu)-P(H)tBu\}]$, and $[Cp(CO)_2W\{P(Cl)-P(Ph)N(SiMe_3)_2\}]$ exhibit slightly longer P1—W1 distances (2.572(2)−2.576(3) Å) and significantly shorter P2—W1 bond lengths (2.335(2)−2.4209(9) Å).[40,41] Interestingly, all the P1 atoms show pyramidal geometries (sum of angles ΣP1 284.1−291.9°), and the P2 atoms are all tetrahedral; however, neglecting the P2—W1 bond, the tBu_2P phosphanyl groups exhibit a high degree of planarity (ΣP2 338.5°−341.7°). The torsion angles of (CH_2)C1—P1—P2—C4(*t*Bu) are in the range from −17.0(6)° to 12.8(3)° and indicate the syn-periplanar orientation of the *t*Bu group and the CH_2 moiety directly bound to the P1 atom; moreover, it points to the presence of a lone pair of electrons on the P1 atom. The analogous ligand geometry was previously observed by us for the methylated phosphanylphosphinidene group in $[(DippN)_2W(X)(1,2\text{-}\eta\text{-}tBu_2P-PCH_3)]$ (X = Cl, I) (**1a**).[35]

In the second part of our study, we investigated the reactivity of platinum phosphanylphosphinidene complexes **2** and **3** toward haloalkanes. The methylation of **2** and **3** by MeI afforded complexes **2a** and **3a**, respectively, bearing tBu_2P-PMe ligands (Scheme 3). In the case of the reaction of **2** with

Scheme 3. Reactions of 2 and 3 with MeI

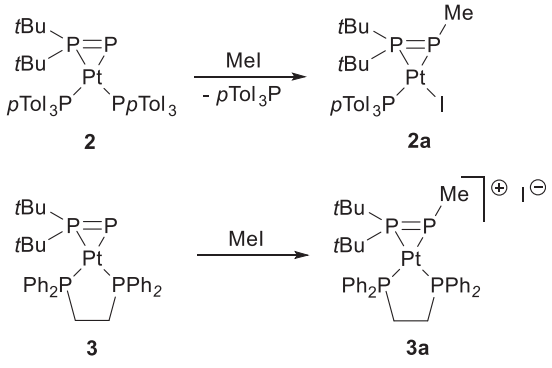

MeI, strong signals of free $pTol_3P$ and resonances of **2a** were observed in the $^{31}P\{^1H\}$ NMR spectra of the reaction mixture. This suggests a replacement of $pTol_3P$ with an iodido ligand in the coordination sphere of platinum. Because of the chelating nature of dppe, such ligand exchange was not observed in the reaction involving **3**, and only cationic complex **3a** was formed. Complex **2a** was isolated in its crystalline form from a toluene solution at low temperature in 49% yield. Because of its ionic character, **3a** exhibits lower solubility in hydrocarbons and was obtained from a THF solution at low temperature in 60% yield.

The reactivities of **2** and **3** toward $I(CH_2)_2I$ differ significantly. According to the $^{31}P\{^1H\}$ NMR spectra of the reaction mixtures, the reaction of **2** with $I(CH_2)_2I$ gave solely new platinum complex **2b** bearing a tBu_2P-P-I ligand together with $pTol_3P$ (Scheme 4A). Moreover, in the ^1H NMR spectrum of this reaction mixture, a resonance at 5.25 ppm attributed to ethylene is present. Complex **2b** was isolated

Scheme 4. Reactions of 2 and 3 with $X(CH_2)_2X$ (X = Br or I)

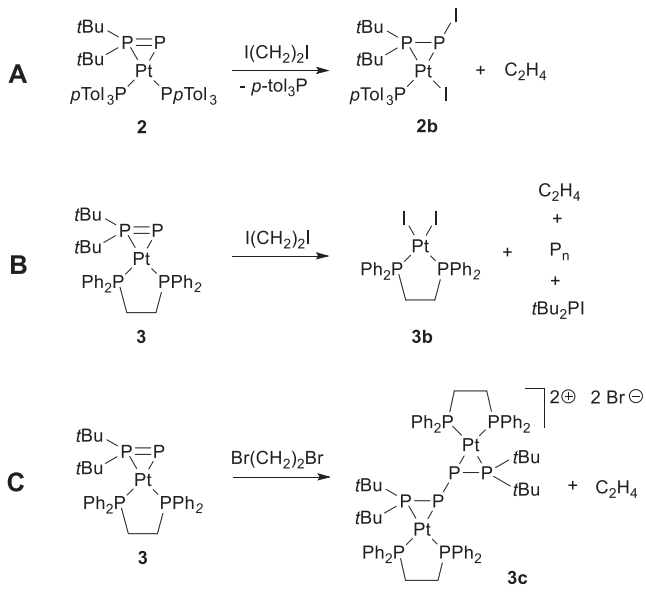

https://dx.doi.org/10.1021/acs.inorgchem.0c00091
Inorg. Chem. 2020, 59, 5463−5474

from a toluene solution at low temperature as brownish crystals in 50% yield. Otherwise, the reaction of **3** with $I(CH_2)_2I$ did not yield the analogous platinum complex. The tBu_2P−P group was lost from the Pt center, and the P—P bond within this ligand was cleaved, resulting in the formation of tBu_2PI, insoluble orange phosphorus polymers, $[(dppe)PtI_2]$ (**3b**)[42] and C_2H_4 (Scheme 4B).

Surprisingly, the reaction of **3** with $Br(CH_2)_2Br$ led to the formation of dimeric platinum complex **3c** (Scheme 4C). This complex features a high-order $^{31}P\{^1H\}$ NMR spectrum with four multiplets at 67.9 ppm (t-Bu_2P), 50.1 ppm (dppe), 47.1 ppm (dppe), and 120.1 ppm (P) (spin system AA′LL′MM′XX′). This suggests the formation of a $tBu_2PPPPtBu_2$ ligand in the coordination sphere of platinum. Complex **3c** exhibits very low solubility in hydrocarbons, but it is highly soluble in dichloromethane (DCM). Crystallization from this solvent layered with toluene at room temperature gave large light-green crystals of **3c** in 27% yield. The reaction of **2** with $Br(CH_2)_2Br$ also gave products with high-order spectra (66.0 ppm (t-Bu_2P), 23.3 ppm (pTol$_3$P), −71.5 ppm (P); AA′MM′XX′ spin system) together with a strong resonance from free pTol$_3$P and other minor unidentified products. This suggests the formation of the same $tBu_2PPPPtBu_2$ ligand, which coordinates to two Pt(pTol$_3$P)Br fragments. However, unlike **3b**, this platinum complex is highly soluble in hydrocarbons, and we were not able to obtain X-ray-quality crystals of this product.

In contrast to reactions of **1** with $Br(CH_2)_nBr$ (n = 3, 4, 6), the analogous reactions involving **2** and **3** gave mostly oily products that were difficult to isolate and characterize. Despite this fact, we were able to obtain crystals of complex **2c** from the reaction of **2** with an equimolar amount of $Br(CH_2)_6Br$ (Scheme 5). The structure of **2c** was unambiguously

Scheme 5. Reactions of 2 with $Br(CH_2)_6Br$

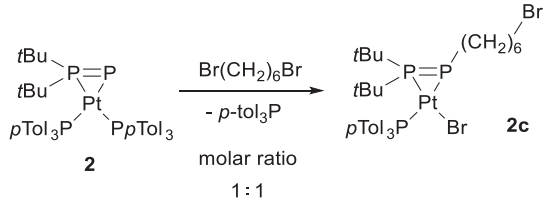

characterized by both NMR spectroscopy and single-crystal X-ray diffraction. $^{31}P\{^1H\}$ NMR spectroscopy showed that the aforementioned reaction is very clean, where **2c** and free pTol$_3$P are the only products.

The $^{31}P\{^1H\}$ NMR data of complexes **2a**−**c**, **3a**, and **3c**, together with corresponding data of parent compounds **2** and **3**, are collected in Table 2.

The comparison of the $^{31}P\{^1H\}$ NMR data of platinum complexes with tBu_2P2−P1−R (R = Me, I, $(CH_2)_6Br$, P−$PtBu_2$) ligands with those of parent compounds **2** and **3** leads to several interesting observations. The $^{31}P\{^1H\}$ spectra of **2a**, **2b**, and **2c** show only three resonances each, which suggests that one phosphine ligand left the coordination sphere of the metal center. On the other hand, the $^{31}P\{^1H\}$ NMR spectra of **3a** and **3c** each contain four resonances, indicating the presence of four inequivalent P atoms in these compounds. In comparison to parent species **2** and **3**, the resonances of P1−R in the aforementioned complexes, except **2b**, which contains a P—I moiety, are strongly upfield shifted, indicating the

Table 2. $^{31}P\{^1H\}$ NMR Data of 2, 3, 2a−c, 3a, and 3c

	chemical shifts [ppm]				coupling constants [Hz]		
compound	(R-)P1	tBu_2P2	R′$_3$P3	R′$_3$P4	$^1J_{P1P2}$ $^2J_{P1P3}$ $^2J_{P1P4}$	$^2J_{P2P3}$ $^2J_{P2P4}$ $^2J_{P3P4}$	$^1J_{P1Pt}$ $^1J_{P2Pt}$ $^1J_{P3Pt}$ $^1J_{P4Pt}$
2	−38.8	77.5	30.5	22.5	615 2 21	206 34 4	52 1906 3452 3397
3	−48.2	71.5	58.3	42.6	622 12 26	214 31 11	116 1894 3358 2915
2a	−97.7	61.2	22.3		483 8	295	349 1653 3623
2b	−30.6	64.2	21.5		520 6	299	170 1598 3523
2c	−68.0	54.8	23.4		483 8	299	432 1694 3606
3a	−130.8	54.5	51.2	49.9	455 36 71	230 24	290 1710 2990 2774
3c	−120.1	67.9	50.1	47.1			416 1696 3052 2854

formation of new P—C (in **2a**, **2c**, and **3a**) or P—P bonds (**3c**). In contrast, the resonances of tBu_2P2 groups in the newly formed Pt complexes are comparable to those observed in parent species **2** and **3**. A strong correlation between $^1J_{P1P2}$ and P—P bond length is observed for phosphanylphosphinidene transition metal complexes.[18] Two extreme examples are side-on platinum complex **2** (large $^1J_{P1P2}$ = 615 Hz and very short P—P bond distance with value of 2.062(2) Å)[12] and terminal zirconium complex $[Cp_2Zr(PPhMe_2)(\eta^1\text{-P}-PtBu_2)]$ (small $^1J_{P1P2}$ = 284 Hz and very long P—P bond distance with a value of 2.20(4) Å).[33] The absolute values of $^1J_{P1P2}$ in **2a**−**c** and **3a** are significantly decreased in comparison to those of **2** and **3**, which suggests elongation of the P—P bond within the ligand. Notably, all resonances for P atoms in **2a**−**c**, **3a**, and **3c** showed platinum satellites.

The small absolute values of $^1J_{P1Pt}$, which are very characteristic of phosphanylphosphinidene complexes **2** and **3**, are significantly increased in the newly formed compounds. Furthermore, the $^1J_{P2Pt}$, $^1J_{P3Pt}$, or $^1J_{P4Pt}$ coupling constants are similar to the corresponding values observed for **2**, **3**, [*trans*-$(R_3P)_2PtCl_2$],[43] and Pt(0) complexes with phosphine ligands.[44] The relatively large absolute value of the $^2J_{P2P3}$ couplings (295−299 Hz) in **2a**−**c** suggests the trans orientation of the tBu_2P1 moiety and the pTol$_3$P3 ligand.

The solid-state structures of platinum complexes **2a**, **2b**, **2c**, **3a**, and **3c** were studied by X-ray diffraction. The molecular structures of these compounds are shown in Figures 3−7. The X-ray studies of **2a**, **2b**, **2c**, **3a**, and **3c** in solution are fully consistent with the NMR data of these complexes. In **2a**, **2b**, **2c**, and **3a**, the tBu_2P−P−R moiety (R = Me (**2a**, **3a**), I (**2b**), $(CH_2)_6Br$ (**2c**)) is side-on coordinated to the Pt center

https://dx.doi.org/10.1021/acs.inorgchem.0c00091
Inorg. Chem. 2020, 59, 5463−5474

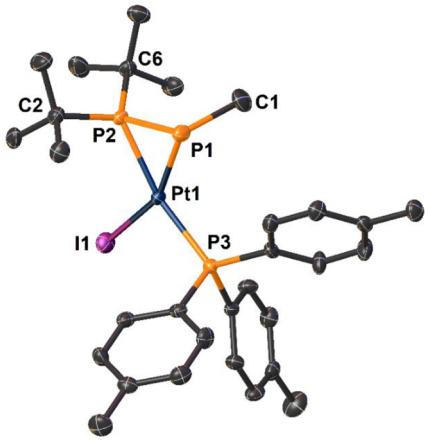

Figure 3. Molecular structure of complex **2a**. Ellipsoids are shown at 50% probability. H atoms are omitted for clarity. Selected bond lengths (Å) and angles (°): P1—Pt1 2.350(2), P2—Pt1 2.285(1), P3—Pt1 2.292(1), I1—Pt1 2.6658(5), P1—P2 2.156(2), C1—P1 1.863(6), ΣP1 278.2, ΣP2 347.1 (neglecting the P2—Pt1 bond), C1—P1—P2 108.6(2), C1—P1—P2—C6 −10.3(3).

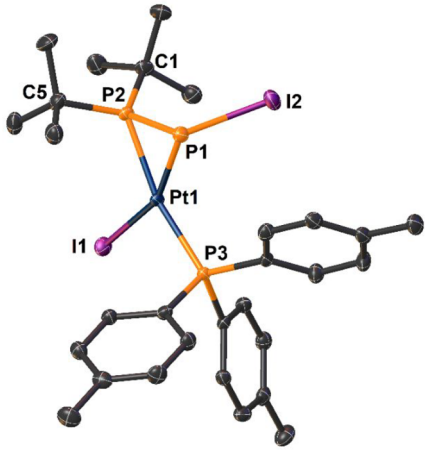

Figure 4. Molecular structure of complex **2b**. Ellipsoids are shown at 50% probability. H atoms are omitted for clarity. Selected bond lengths (Å) and angles (°): P1—Pt1 2.310(1), P2—Pt1 2.282(1), P3—Pt1 2.3004(9), I1—Pt1 2.6551(5), P1—P2 2.173(1), I2—P1 2.491(1), ΣP1 280.4, ΣP2 347.2 (neglecting the P2—Pt1 bond), I2—P1—P2 109.57(5), I2—P1—P2—C1 −7.9(2).

(Figures 3–6), and the metal atom is tetracoordinated with a planar geometry. In **2a–c**, in accordance with the ^{31}P NMR data, the *p*Tol$_3$P ligand and *t*Bu$_2$P are in a trans orientation. Surprisingly, the geometries of the *t*Bu$_2$P–P–R ligands in **2a–c** and **3a** resemble those observed for tungsten complexes **1a–e**: (i) the *t*Bu$_2$P group displays a high degree of planarity (ΣP2: 345.4° to 347.2°); (ii) the P—P bonds have lengths in between the lengths typical of single and double bonds (2.149(3) Å to 2.173(1) Å) and are significantly longer than P—P bonds in precursor complexes **2** (2.062(2) Å)[12] and **3** (2.072(3) Å);[13] (iii) the angles P2—P1—R have values in a narrow range of 108.6(2)° to 110.1(3)°; (iv) one of the *t*Bu groups is syn-periplanar with respect to the R group with torsion angles for C(*t*Bu)–P2—P1—R from −12.5(5)° to 8.3(4)°.

Unlike tungsten complexes **1a–c** and **1e**, in the aforementioned platinum complexes significant elongation of the P1—M1 bond resulting from the attachment of the R group to

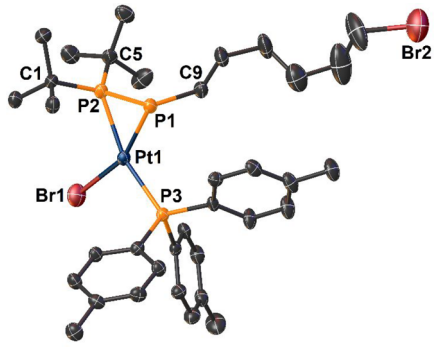

Figure 5. Molecular structure of complex **2c**. Ellipsoids are shown at 50% probability. H atoms are omitted for clarity. Selected bond lengths (Å) and angles (°): P1—Pt1 2.322(3), P2—Pt1 2.282(2), P3—Pt1 2.283(2), Br1—Pt1 2.519(1), P1—P2 2.149(3), C9—P1 1.87(1), ΣP1 278.0, ΣP2 347.2 (neglecting the P2—Pt1 bond), C9—P1—P2 109.6(3), C9—P1—P2—C5 −12.5(5).

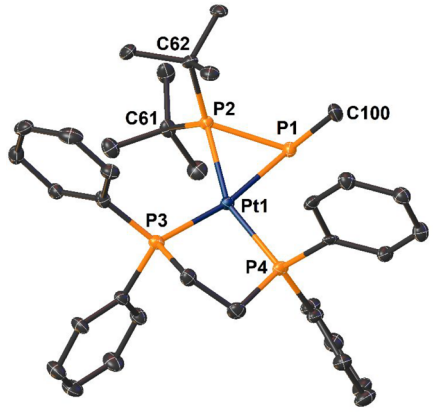

Figure 6. Molecular structure of complex cation **3a**. One molecule out of the three present in the asymmetric unit was selected. Ellipsoids are shown at 50% probability. H atoms, solvent molecules, and iodide anion are omitted for clarity. Selected bond lengths (Å) and angles (°): P1—Pt1 2.406(2), P2—Pt1 2.285(2), P3—Pt1 2.274(2), P4—Pt1 2.274(2), P1—P2 2.157(3), C100—P1 1.862(8), ΣP1 278.5, ΣP2 345.4 (neglecting the P2—Pt1 bond), C100—P1—P2 108.6(2), C100—P1—P2–C62 8.3(4).

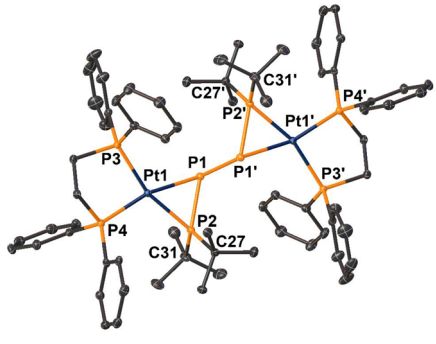

Figure 7. Molecular structure of complex dication **3c**. Ellipsoids are shown at 50% probability. H atoms and bromide anions are omitted for clarity. Selected bond lengths (Å) and angles (°): P1—Pt1 2.415(1), P2—Pt1 2.287(1), P3—Pt1 2.304(1), P4—Pt1 2.275(1), P1—P2 2.165(1), P1—P1′ 2.235(1), ΣP1 277.8, ΣP2 346.8 (neglecting the P2—Pt1 bond), P2—P1—P1′ 106.34(5), P2—P1—P1′—P2′ 180 (centrosymmetric structure).

https://dx.doi.org/10.1021/acs.inorgchem.0c00091
Inorg. Chem. 2020, 59, 5463–5474

Table 3. Calculated Hirshfeld Charges (q) and Wiberg Bond Indexes for Complexes 1a, 2a, 2b, and 3c

	Hirshfeld charges			Wiberg bond indexes			
compound	q(P2)	q(P1)	q(M1)	P1—P2	P1—P1′	P1—M	P2—M
1a	0.194	0.057	0.431	1.002		0.727	0.511
2a	0.208	0.033	0.030	1.116		0.510	0.490
2b	0.205	0.004	0.043	1.093		0.556	0.479
3c′	0.193	−0.023	0.035	1.089	0.983	0.412	0.461

Table 4. Calculated Hirshfeld Charges (q) and Optimized Parameters for Free Phosphenium Cations I–III[a]

cation	q(P2)	q(P1)	P1—P2 (Å)	P1—P1′ (Å)	ΣP2 (°)	P2—P1—R (°)
I (tBu$_2$P$^+$=P-Me)	0.304	0.220	2.036		359.3	107.4
			(**1a**: 2.160) (**2a**: 2.156)		(**1a**: 341.7) (**2a**: 347.1)	(**1a**: 109.9) (**2a**: 108.6)
II (tBu$_2$P$^+$=P—I)	0.294	0.168	2.055		359.3	109.0
			(**2b**: 2.173)		(**2b**: 347.2)	(**2b**: 109.6)
III ((tBu$_2$P$^+$=P)$_2$)	0.345	0.140	2.057	2.224	359.9	102.4
			(**3c**: 2.165)	(**3c**: 2.235)	(**3c**: 346.8)	(**3c**: 106.3)

[a]Values in parentheses are experimental parameters for the corresponding ligands in **1a**, **2a**, **2b**, and **3c**.

the P1 atom was not observed. The P1—Pt1 distances in **2a–c** (2.310(1) Å to 2.350(2) Å) are even shorter than that in parent species **2** (2.409(2) Å), whereas in **3a**, the P1—Pt1 bond length (2.406(2) Å) is very similar to the corresponding distance in **3** (2.387(2) Å). The P2—Pt1, P3—Pt1, and P4—Pt1 distances are comparable to those observed in platinum complexes with phosphine ligands.[45]

The molecular structure of complex dication **3c** is presented in Figure 7. It consists of tetraphosphorus ligand tBu$_2$P2—P1—P1′—P2′tBu$_2$ and two dppe ligands that coordinate to two platinum centers. Additionally, two bromide counterions are present in the second coordination sphere (not shown in Figure 7).

The metal centers show square planar geometries and the whole molecule is centrosymmetric (point group C_i). As a consequence, the P2—P1—P1′—P2′ bonds lie in the same plane with a corresponding torsion angle of 180° and the two (dppe)Pt moieties are located on opposite sides of this plane. The P1—P1′ bond (2.235(1) Å) has a length typical of a single covalent P—P bond, whereas the P2—P1 and P2′—P1′ bonds are 0.07 Å shorter. The platinum—phosphorus bonds in **3c** and in parent complex **3** have very similar lengths. Dimeric molybdenum and tungsten complexes with analogous tBu$_2$PPPPtBu$_2$ ligands were previously synthesized by our group from the reaction of Li[Cp*(CO)$_3$] with tBu$_2$P–PCl$_2$.[46] The tetraphosphorus ligands in these complexes displayed geometries very similar to the corresponding ligand in **3c**.

We performed DFT calculations (see SI for details) to further elucidate the electronic structures of the obtained tungsten and platinum complexes. As presented in the previous paragraphs, W or Pt complexes with tBu$_2$P–P–R exhibit many common structural features. Therefore, for this study we selected representative complexes **1a**, **2a** (tBu$_2$P–P–Me ligand), and **2b** (tBu$_2$P–P–I ligand). Moreover, we studied the electronic properties of complex **3c′** (tBu$_2$P–P–P–PtBu$_2$ ligand) with a skeleton similar to that of **3c** in which the dppe ligands were replaced by dmpe (Me$_2$PCH$_2$CH$_2$PMe$_2$) groups to simplify the calculations. Our previous theoretical studies on tungsten complex **1** revealed that the P1—P2 bond within the tBu$_2$P2–P1 ligand is polarized toward the phosphinidene P1-atom. Furthermore, the P1—P2 and P2—W1 bonds are essentially single bonds, whereas the P1—W1 bond has double bond character. Moreover, a lone electron pair is present on the P1 atom. In the case of Pt complex **2**, similar to **1**, the phosphanylphosphinidene ligand displays a positively charged P2 atom and a negatively charged P1 atom. In contrast to **1**, Pt complex **2** exhibits a P1=P2 double bond and has two lone pairs on the P1 atom.[18] NBO analysis of complexes **1a**, **2a**, and **2b** indicates that the P1—P2 bond within the tBu$_2$P–P–R ligand as well as the P1—M1 and P2—M1 bonds have single-bond character. The mentioned complexes display one lone pair of electrons on the P1 atom. The shortening of the P1—P2 bonds in **1a**, **2a**, and **2b** can be explained by the interactions of the antibonding σ^*(P2–C) orbitals with the orbital attributed to the lone pair on the P1 atom (negative hyperconjugation). The analysis of the Hirshfeld charges of complexes **1a**, **2a**, and **2b** revealed that the positive charge is located on the P2 atom of the phosphanyl group, whereas the charge on the P1 atom is close to zero (Table 3). Moreover, the W1 atom in **1a** is positively charged, whereas the charges on the Pt1 atoms in **2a** and **2b** are close to zero. As it can be expected, in the case of **1a** significant negative charges are located on imido and chlorido ligands, as well as methyl group bound to P1 atom (Figure S72). In complexes **2a** and **2b**, negative charge is located primarily on iodido ligands and on the methyl group (**2a**) or iodine atom (**2b**) directly bound to P1 atom (Figures S73 and S74). These results indicate that the phosphorus ligands in **1a**, **2a**, and **2b** can be seen as coordinated diphosphenium cations tBu$_2$P$^+$=P–R resulting formally from the reaction of the tBu$_2$P–P group with the R$^+$ cation. A similar bonding mode is observed in complex **3c**, where dicationic tBu$_2$P$^+$=P–P=P^+tBu$_2$ ligand coordinates to two platinum metal centers. Notably, based on our previous calculations, the phosphorus ligands in dimeric complexes [Cp*M(CO)$_3$(η^2-tBu$_2$PP)]$_2$ (M = Mo, W) possess analogous Lewis structures.[46]

Consequently, we performed analogous calculations for free phosphenium cations tBu$_2$P$^+$=P–Me (**I**),tBu$_2$P$^+$=P–I (**II**) and (tBu$_2$P$^+$=P)$_2$ (**III**). On the basis of our calculations, these species have a singlet ground state. The optimized structures of **I–III** are presented in Figures S66, S70, and S71, and their selected optimized parameters together with Hirshfeld charges are collected in Table 4.

As expected, the P atoms in **I-III** are positively charged with a large charge on the P2 atom and a smaller positive charge on the P1 atom. A comparison of the geometries of **I-III** with the

https://dx.doi.org/10.1021/acs.inorgchem.0c00091
Inorg. Chem. 2020, 59, 5463–5474

geometries of the corresponding ligands in **1a**, **2a**, **2b**, and **2c** reveals several similarities, such as the planar geometric alignment of the tBu$_2$P2 phosphanyl group, the very close values of the P2—P1—R angles, and the same syn-periplanar conformation (Table 4). Similar structural features also include the isolated, noncoordinated diphosphenium cation Mes*-(Me)P$^+$=PMes*.[47] However, in comparison to the corresponding ligands in the W and Pt complexes, the P1—P2 bonds in **I**–**III** are significantly shorter and have double bond character. This important structural difference can be explained by considering the complexation of these cationic ligands to the metal center. In free ligands **I**–**III**, the lone pair on the P2 atom (tBu$_2$P group) is mainly involved in P—P π-bonding, whereas in the corresponding complexes, this lone pair interacts with the metal center.

3. CONCLUSIONS

Our studies showed that phosphanylphosphinidene complexes of tungsten and platinum are valuable substrates in the synthesis of not only new diphosphorus ligand species but also new polydentate phosphorus ligands. The reactions of complexes [(DippN)$_2$W(Cl)(η^2-P−PtBu$_2$)]$^-$ (**1**), [(pTol$_3$P)$_2$Pt(η^2-P=PtBu$_2$)] (**2**), and [(dppe)Pt(η^2-P=PtBu$_2$)] (**3**) with MeI and haloalkanes gave a wide range of transition metal complexes bearing ligands with two or four P-donor atoms. Nucleophilic **1** is very reactive toward Br(CH$_2$)$_n$Br (n = 3, 4, 6), forming unprecedented dinuclear complexes bearing tetradentate ligands where two tBu$_2$P−P groups are linked by an aliphatic chain (n = 4, 6) or monometallic complexes with a tBu$_2$P−P(CH$_2$)$_3$Br ligand. The reactions of platinum complexes with MeI and dihaloalkanes gave even more diverse compounds. We showed that the tBu$_2$P−P ligand in the starting platinum complexes can be easily functionalized by introducing a wide range of substituents on terminal P-phosphinidene atoms, such as halogen atoms, Me, (CH$_2$)$_n$Br or P−PtBu$_2$ groups. Despite the diversity of functionalized phosphanylphosphinidene ligands, they exhibit many structural similarities and can be described as phosphenium cations tBu$_2$P$^+$=P − R or (tBu$_2$P$^+$=P)$_2$. In summary, the presented results may be of importance in the synthesis of polydentate phosphorus ligands coordinated to TM with possible catalytic activity.

4. EXPERIMENTAL SECTION

General Information. All experiments were carried out under an argon atmosphere using Schlenk techniques. All manipulations were performed using standard vacuum, Schlenk, and glovebox techniques. All solvents were purified and dried using common methods. Solvents for NMR spectroscopy (C_6D_6 and $CDCl_3$) were purified from metallic sodium or P_2O_5. The phosphanylphosphinidene tungsten complex [(2,6-iPr$_2$C$_6$H$_3$N)$_2$(Cl)W(η^2-tBu$_2$P−P)]Li·3DME (**1**)[11] and phosphanylphosphinidene platinum complex [(pTol$_3$P)$_2$Pt(η^2-tBu$_2$P=P)] (**2**)[12] were synthesized following literature methods. Methyl iodide, 1,2-diiodoethane, 1,2-dibromoethane, 1,3-dibromopropane, 1,4-dibromobutane and 1,6-dibromohexane were purchased from commercial sources. All of the solutions of dibromoalkanes, methyl iodide, and 1,2-diiodoethane used in this work were freshly prepared prior to use. NMR spectra were recorded on a Bruker Avance III HD 400 MHz spectrometer at ambient temperature (external standards: TMS for ^{1}H and ^{13}C; 85% H_3PO_4 for ^{31}P). The chemical shifts of C_i and CH_2 in some cases were not determined due to the absence of these signals in the ^{13}C{^{1}H} NMR spectra. The Cl/Br ratio in the case of tungsten complexes was determined on the basis of the ^{31}P NMR spectra. Crystallographic analyses were performed on an STOE IPDS II diffractometer using MoKα radiation (λ = 0.71073 Å). Elemental analyses were performed at the University of Gdańsk using a Vario El Cube CHNS apparatus.

Synthesis of 1b. To a solution of **1** (0.512 g, 0.500 mmol) in 4 mL of DME was dropwise added 0.873 mL of a solution of 1,3-dibromopropane (0.500 mmol, C_M = 0.573 M) at −30 °C. After warming to room temperature, NMR spectra were collected every 5 min for 30 min. The reaction was complete after this time. The solvent was evaporated, the solid residue was redissolved in pentane, and the LiBr precipitate was removed by filtration. Yellow crystals of **1b-Cl**/**1b-Br** (0.213 g, 0.240 mmol, yield 48%, molar ratio **1b-Cl**/**1b-Br** equals 0.6:0.4 on the basis of the ^{31}P NMR spectrum) were obtained from the pentane filtrate at −30 °C. Mixing in C_6D_6 or DME and heating overnight at 50 °C did not result in the formation of a compound analogous to **1d**.

NMR data for **1b**:

^{1}H NMR (C_6D_6, 400 MHz, 298 K δ): 1.22 (broad s, 12H, HC(C**H**$_3$)$_2$), 1.27 (d, $^3J_{HH}$ = 7 Hz, 6H, HC(C**H**$_3$)$_2$), 1.28 (d, $^3J_{HH}$ = 7 Hz, 6H, HC(C**H**$_3$)$_2$), 1.35 (d, $^3J_{PH}$ = 16 Hz, 18H, C(C**H**$_3$)$_3$), 1.82 (m, 2H, PC**H**$_2$), 2.44 (m, 2H, C**H**$_2$), 2.89 (m, 2H, C**H**$_2$Br), 4.09 (m, 4H, **H**C(CH$_3$)$_2$), 6.97 (m, 2H, C$_{Ar}$−**H**$_p$), 7.07 (m, overlapped, 4H, C$_{Ar}$−**H**$_m$).

1b-Cl: ^{31}P{^{1}H} NMR (C_6D_6, 162 MHz, 298 K, δ): 40.0 (d, $^1J_{PP}$ = 375 Hz, $^1J_{PW}$ = 17 Hz, tBu$_2$**P**), −125.3 (d, $^1J_{PP}$ = 375 Hz, $^1J_{PW}$ = 80 Hz, **P**(CH$_2$)$_3$Br).

1b-Br: ^{31}P{^{1}H} NMR (C_6D_6, 162 MHz, 298 K, δ): 36.9 (d, $^1J_{PP}$ = 381 Hz, $^1J_{PW}$ = 17 Hz, tBu$_2$**P**), −132.2 (d, $^1J_{PP}$ = 381 Hz, $^1J_{PW}$ = 80 Hz, **P**(CH$_2$)$_3$Br).

^{13}C{^{1}H} NMR (C_6D_6, 100 MHz, 298 K δ): 22.8 (dd, $^1J_{CP}$= 44 Hz, $^2J_{CP}$= 4 Hz, P**C**H$_2$), 23.7 (broad s, HC(**C**H$_3$)$_2$), 23.8 (broad s, HC(**C**H$_3$)$_2$), 24.1 (broad s, HC(**C**H$_3$)$_2$), 27.9 (m, H**C**(CH$_3$)$_2$), 31.6 (broad s, C(**C**H$_3$)$_3$), 32.8 (m, **C**H$_2$), 35.1 (m, Br**C**H$_2$), 37.6 (very broad s, **C**(CH$_3$)$_3$), 122.4 (s, **C**$_m$), 122.5 (s, **C**$_m$), 125.8 (broad s, **C**$_p$), 144.3 (m, overlapped, **C**$_o$), 152.3 (m, overlapped, **C**$_i$).

Elemental analysis calculated for $C_{35}H_{58}Br_{1.4}Cl_{0.6}N_2P_2W$ (M = 885.77 g/mol): % C = 47.46%, % H = 6.60%, % N = 3.16%; found % C = 47.55%, % H = 6.70%, % N = 3.15%.

Synthesis of 1c. To a solution of **1** (0.506 g, 0.494 mmol) in 4 mL of DME was dropwise added 1.29 mL of a solution of 1,4-dibromobutane (0.494 mmol, C_M = 0.383 M) at −30 °C. After warming to room temperature, NMR spectra were collected every 5 min for 30 min. The solvent was evaporated, the solid residue was redissolved in pentane, and the LiBr precipitate was removed by filtration. Yellow crystals of **1c-Cl**/**1c-Br** (0.133 g, 0.084 mmol, yield 34.1%, molar ratio **1c-Cl**/**1c-Br** equals 1.3:0.7 on the basis of the ^{31}P NMR spectrum) were obtained from the pentane filtrate at −30 °C. Crystals for NMR spectroscopy and elemental analysis were obtained from a toluene solution at −30 °C, and the crystals contain two molecules of toluene in the structure.

NMR data for **1c**:

^{1}H NMR (C_6D_6, 400 MHz, 298 K δ): 1.23 (very broad s, overlapped, 24H, HC(C**H**$_3$)$_2$), 1.28 (d, overlapped, $^3J_{HH}$ = 7 Hz, 24H, HC(C**H**$_3$)$_2$), 1.38 (d, $^3J_{PH}$ = 16 Hz, 36H, C(C**H**$_3$)$_3$), 1.55 (broad m, 4H, PC**H**$_2$), 2.32 (m, 4H, C**H**$_2$), 4.11 (very broad s, 8H, **H**C(CH$_3$)$_2$), 6.98 (m, 4H, C$_{Ar}$−**H**$_p$), 7.07 (m, overlapped, 8H, C$_{Ar}$−**H**$_m$).

1c-Cl: ^{31}P{^{1}H} NMR (C_6D_6, 162 MHz, 298 K, δ): 40.3 (d, $^1J_{PP}$ = 378 Hz, $^1J_{PW}$ = 17 Hz, tBu$_2$**P**), −122.2 (d, $^1J_{PP}$ = 378 Hz, $^1J_{PW}$ = 76 Hz, **P**(CH$_2$)$_4$).

1c-Br: ^{31}P{^{1}H} NMR (C_6D_6, 162 MHz, 298 K, δ): 37.2 (d, $^1J_{PP}$ = 383 Hz, $^1J_{PW}$ = 17 Hz, tBu$_2$**P**), −129.1 (d, $^1J_{PP}$ = 383 Hz, $^1J_{PW}$ = 80 Hz, **P**(CH$_2$)$_4$).

^{13}C{^{1}H} NMR (C_6D_6, 100 MHz, 298 K δ): 23.7 (broad s, HC(**C**H$_3$)$_2$), 23.8 (broad s, HC(**C**H$_3$)$_2$), 24.2 (broad s, HC(**C**H$_3$)$_2$), 27.8 (m, overlapped, H**C**(CH$_3$)$_2$), 31.6 (broad s, (C(**C**H$_3$)$_3$), 37.4 (broad s, **C**(CH$_3$)$_3$), 122.4 (s, **C**$_m$), 122.5 (s, **C**$_m$), 125.7 (broad s, **C**$_p$), 144.2 (m, overlapped, **C**$_o$), 152.3 (m, overlapped, **C**$_i$), CH$_2$− are not visible due to the broadness.

Elemental analysis calculated for $C_{82}H_{128}Br_{0.5}Cl_{1.5}N_4P_4W_2$ (M = 1754.63 g/mol): % C = 56.13%, % H = 7.35%, % N = 3.19%; found % C = 56.03%, % H = 7.26%, % N = 3.18%.

https://dx.doi.org/10.1021/acs.inorgchem.0c00091
Inorg. Chem. 2020, 59, 5463−5474

Synthesis of 1d. The reaction was conducted using the same amounts of reactants as were used to synthesize **1c-Cl/1c-Br** at room temperature, and after 3 days almost all **1c-Cl/1c-Br** was gone and **1d** was formed along with $[(2,6\text{-}i\mathrm{Pr}_2\mathrm{C}_6\mathrm{H}_3\mathrm{N})_2\mathrm{WX}_2\cdot\mathrm{DME}$ (X = Cl, Br). The molar ratio of the products (**1d/1c**) was 2.3:1 based on the $^{31}\mathrm{P}\{^1\mathrm{H}\}$ NMR spectrum (70% **1d** and 30% **1c-Cl/1c-Br**, not taking into account other products of this reaction).

NMR data for **1d**:

^{1}H NMR ($\mathrm{C_6D_6}$, 400 MHz, 298 K δ): 1.24 (d, $^3J_{\mathrm{PH}}$ = 7 Hz, 18H, $\mathrm{C(CH_3)_3}$), 1.54 (m, 4H, $\mathrm{CH_2}$), 1.77 (m, 4H, $\mathrm{CH_2}$).

$^{31}\mathrm{P}\{^1\mathrm{H}\}$ NMR ($\mathrm{C_6D_6}$, 162 MHz, 298 K, δ): δ 42.3 (d, $^1J_{\mathrm{PP}}$ = 203 Hz, $t\mathrm{Bu_2P}$), −37.3 (d, $^1J_{\mathrm{PP}}$ = 203 Hz, $\mathrm{P(CH_2)_4}$).

$^{13}\mathrm{C}\{^1\mathrm{H}\}$ NMR ($\mathrm{C_6D_6}$, 100 MHz, 298 K δ): 26.2 (dd, $^1J_{\mathrm{CP}}$ = 18 Hz, $^2J_{\mathrm{CP}}$ = 13 Hz, $\mathrm{PCH_2}$), 28.6 (broad s, $\mathrm{CH_2}$), 31.6 (broad s, $\mathrm{(C(CH_3)_3)}$, 32.8 (dd, $^1J_{\mathrm{CP}}$ = 30 Hz, $^2J_{\mathrm{CP}}$ = 7 Hz, $\mathrm{C(CH_3)_3}$).

Synthesis of 1e. To a solution of **1** (0.493 g, 0.480 mmol) in DME was dropwise added 1.68 mL of a solution of 1,6-dibromohexane (0.480 mmol, C_{M} = 0.286 M) at −30 °C. After warming to room temperature, NMR spectra were collected every 5 min for 30 min. The solvent was evaporated, and the solid residue was redissolved in pentane. Colorless crystals of **1e-Cl/1e-Br** (0.162 g, 0.101 mmol, yield 42%, molar ratio **1e-Cl/1e-Br** equals 1.3:0.7 on the basis of the ^{31}P NMR spectrum) were grown at −30 °C. Adding the reactants in the reverse manner results in the same NMR spectra and crystalline product. No formation of a compound analogous to **1d** was observed at RT.

NMR data for **1e**:

^{1}H NMR ($\mathrm{C_6D_6}$, 400 MHz, 298 K δ): 0.99 (broad m, overlapped, 4H, $\mathrm{PCH_2}$), 1.25 (broad s, overlapped, 4H, $\mathrm{CH_2}$), 1.25 (very broad s, 18H, $\mathrm{HC(CH_3)_2}$), 1.30 (d, overlapped, 30H, $^3J_{\mathrm{HH}}$ = 7 Hz, $\mathrm{HC(CH_3)_2}$), 1.40 (d, 36H, $^3J_{\mathrm{PH}}$ = 16 Hz, $\mathrm{C(CH_3)_3}$), 2.38 (m, 4H, $\mathrm{CH_2}$), 4.14 (m, 8H, $\mathrm{HC(CH_3)_2}$), 6.97 (m, 4H, $\mathrm{C_{Ar}}$−$\mathrm{H_p}$), 7.08 (m, overlapped, 8H, $\mathrm{C_{Ar}}$−$\mathrm{H_m}$).

1e-Cl: $^{31}\mathrm{P}\{^1\mathrm{H}\}$ NMR ($\mathrm{C_6D_6}$, 162 MHz, 298 K, δ): 40.5 (d, $^1J_{\mathrm{PP}}$ = 378 Hz, $^1J_{\mathrm{PW}}$ = 18 Hz, $t\mathrm{Bu_2P}$), −122.1 (d, $^1J_{\mathrm{PP}}$ = 378 Hz, $^1J_{\mathrm{PW}}$ = 80 Hz, $\mathrm{P(CH_2)_6}$).

1e-Br: $^{31}\mathrm{P}\{^1\mathrm{H}\}$ NMR ($\mathrm{C_6D_6}$, 162 MHz, 298 K, δ): 37.4 (d, $^1J_{\mathrm{PP}}$ = 382 Hz, $^1J_{\mathrm{PW}}$ = 18 Hz, $t\mathrm{Bu_2P}$), −129.0 (d, $^1J_{\mathrm{PP}}$ = 382 Hz, $^1J_{\mathrm{PW}}$ = 80 Hz, $\mathrm{P(CH_2)_6}$).

$^{13}\mathrm{C}\{^1\mathrm{H}\}$ NMR ($\mathrm{C_6D_6}$, 100 MHz, 298 K δ): 23.8 (broad s, $\mathrm{HC(CH_3)_2}$), 23.9 (broad s, $\mathrm{HC(CH_3)_2}$), 24.2 (broad s, $\mathrm{HC(CH_3)_2}$), 24.2 (dd, $^1J_{\mathrm{CP}}$ = 44 Hz, $^2J_{\mathrm{CP}}$ = 6 Hz, $\mathrm{PCH_2}$), 27.8 (s, overlapped, $\mathrm{HC(CH_3)_2}$), 27.9 (s, overlapped, $\mathrm{HC(CH_3)_2}$), 30.4 (m, $\mathrm{CH_2}$), 31.7 (broad s, $\mathrm{C(CH_3)_3}$), 32.7 (m, $\mathrm{CH_2}$), 37.5 (broad s, $\mathrm{C(CH_3)_3}$), 122.4 (s, $\mathrm{C_m}$), 122.5 (s, $\mathrm{C_m}$), 125.7 (broad s, $\mathrm{C_p}$), 144.4 (m, overlapped, $\mathrm{C_o}$), 152.5 (m, overlapped, $\mathrm{C_i}$).

Additionally, the signals attributable to pentane are visible in the ^{1}H and $^{13}\mathrm{C}\{^1\mathrm{H}\}$ NMR spectra.

Elemental analysis calculated for (**1e**·pentane): $\mathrm{C_{75}H_{128}Br_{0.7}Cl_{1.3}N_4P_4W_2}$ (M = 1679.44 g/mol): % C = 53.64%, % H = 7.68%, % N = 3.34%; found % C = 53.41%, % H = 7.80%, % N = 3.13%.

Synthesis of 2a. To a suspension of **2** (0.379 g, 0.383 mmol) in toluene was dropwise added 0.586 mL of a solution of methyl iodide (0.383 mmol, C_{M} = 0.653 M) at −30 °C. The reaction was complete after 1 h, which was confirmed by NMR spectroscopy. The solvent was evaporated, and the solid residue was dissolved partially in pentane and the rest in toluene. Colorless crystals of **2a** were obtained from both fractions at −30 °C but they were contaminated with $p\mathrm{Tol_3P}$ (the crystals obtained from toluene were much less contaminated than those from pentane). The yield of crystals from the toluene fraction was 49.2% (0.154 g, 0.188 mmol).

NMR data for **2a**:

^{1}H NMR ($\mathrm{C_6D_6}$, 400 MHz, 298 K δ): 0.73 (m, 3H, $\mathrm{H_3C}$−P), 1.35 (d, $^3J_{\mathrm{PH}}$ = 16 Hz, 9H, $\mathrm{C(CH_3)_3}$), 1.37 (d, $^3J_{\mathrm{PH}}$ = 16 Hz, 9H, $\mathrm{C(CH_3)_3}$), 1.93 (s, 9H, $p\text{-}\mathrm{CH_3}\text{-}\mathrm{C_6H_4}$), 6.90 (d, $^3J_{\mathrm{HH}}$ = 7 Hz, 6H, $\mathrm{C_{Ar}}$−$\mathrm{H_m}$), 7.80 (m, 6H, $\mathrm{C_{Ar}}$−$\mathrm{H_o}$).

$^{31}\mathrm{P}\{^1\mathrm{H}\}$ NMR ($\mathrm{C_6D_6}$, 162 MHz, 298 K, δ): 61.2 (dd, $^1J_{\mathrm{PP}}$ = 483 Hz, $^2J_{\mathrm{PP}}$ = 295 Hz, $^1J_{\mathrm{PPt}}$ = 1653 Hz, $t\mathrm{Bu_2P}$), 22.3 (dd, $^2J_{\mathrm{PP}}$ = 295 Hz, $^2J_{\mathrm{PP}}$ = 8 Hz, $^1J_{\mathrm{PPt}}$ = 3623, $p\mathrm{Tol_3P}$), −97.7 (dd, $^1J_{\mathrm{PP}}$ = 483 Hz, $^2J_{\mathrm{PP}}$ = 8 Hz, $^1J_{\mathrm{PPt}}$ = 349 Hz, PMe), weak signal of $p\mathrm{Tol_3P}$ (s, −7.9 ppm) was visible.

$^{13}\mathrm{C}\{^1\mathrm{H}\}$ NMR ($\mathrm{C_6D_6}$, 100 MHz, 298 K δ): 3.7 (dd, $^1J_{\mathrm{CP}}$ = 55 Hz, $^2J_{\mathrm{CP}}$ = 7 Hz, $\mathrm{H_3C}$-P), 20.8 (s, $p\text{-}\mathrm{CH_3}\text{−}\mathrm{C_6H_4}$), 31.8 (d, $^2J_{\mathrm{CP}}$ = 8 Hz, $\mathrm{C(CH_3)_3}$), 32.2 (m, $\mathrm{C(CH_3)_3}$), 36.1 (m, $\mathrm{C(CH_3)_3}$), 37.2 (m, $\mathrm{C(CH_3)_3}$), 128.9 (d, $^3J_{\mathrm{CP}}$ = 10 Hz, $\mathrm{C_m}$), 130.8 (dd, $^1J_{\mathrm{CP}}$ = 51 Hz, $^3J_{\mathrm{CP}}$ = 2 Hz, $\mathrm{C_i}$), 134.5 (d, $^2J_{\mathrm{CP}}$ = 12 Hz, $\mathrm{C_o}$), 139.9 (d, $^4J_{\mathrm{CP}}$ = 2 Hz, $\mathrm{C_p}$).

Elemental analysis calculated for $\mathrm{C_{30}H_{42}IP_3Pt}$ (M = 817.5642 g/mol): % C = 44.07%, % H = 5.18%, found % C= 44.84%, % H = 5.23%

Synthesis of 2b. To a suspension of **2** (0.418 g, 0.422 mmol) in toluene was dropwise added a solution of 1,2-diiodoethane (0.119 g, 0.422 mmol) in 1 mL of toluene at −30 °C. The reaction was complete after 2 h, which was confirmed by NMR spectroscopy. Light-brown crystals of **2b** (0.198 g, 0.213 mmol, yield 50.5%) were obtained from a toluene solution at −30 °C.

NMR data for **2b**:

^{1}H NMR ($\mathrm{C_6D_6}$, 400 MHz, 298 K δ): 1.24 (d, $^3J_{\mathrm{PH}}$ = 16 Hz, 9H, $\mathrm{(CH_3)_3C}$), 1.68 (d, $^3J_{\mathrm{PH}}$ = 17 Hz, 9H, $\mathrm{(CH_3)_3C}$), 1.99 (s, 9H, $p\text{-}\mathrm{CH_3}\text{−}\mathrm{C_6H_4}$), 6.97 (d, $^3J_{\mathrm{HH}}$ = 7 Hz, 6H, $\mathrm{C_{Ar}}$−$\mathrm{H_m}$), 7.87 (m, 6H, $\mathrm{C_{Ar}}$−$\mathrm{H_o}$).

$^{31}\mathrm{P}\{^1\mathrm{H}\}$ NMR ($\mathrm{C_6D_6}$, 162 MHz, 298 K, δ): 64.2 (dd, $^1J_{\mathrm{PP}}$ = 520 Hz, $^2J_{\mathrm{PP}}$ = 299 Hz, $^1J_{\mathrm{PPt}}$ = 1598 Hz, $t\mathrm{Bu_2P}$), 21.5 (dd, $^2J_{\mathrm{PP}}$ = 299 Hz, $^2J_{\mathrm{PP}}$ = 6 Hz, $^1J_{\mathrm{PPt}}$ = 3523, $p\mathrm{Tol_3P}$), −30.6 (dd, $^1J_{\mathrm{PP}}$ = 520 Hz, $^2J_{\mathrm{PP}}$ = 6 Hz, $^1J_{\mathrm{PPt}}$ = 170 Hz, PI).

$^{13}\mathrm{C}\{^1\mathrm{H}\}$ NMR ($\mathrm{C_6D_6}$, 100 MHz, 298 K δ): 20.8 (s, $p\text{-}\mathrm{CH_3}\text{−}\mathrm{C_6H_4}$), 31.6 (m, overlapped, $\mathrm{(CH_3)_3C}$), 37.8 (m, $\mathrm{(CH_3)_3C}$), 39.2 (m, $\mathrm{(CH_3)_3C}$), 129.1 (d, $^3J_{\mathrm{CP}}$ = 11 Hz, $\mathrm{C_m}$), 134.6 (d, $^2J_{\mathrm{CP}}$ = 11 Hz, $\mathrm{C_o}$), 140.3 (d, $^4J_{\mathrm{CP}}$ = 2 Hz, $\mathrm{C_p}$), $\mathrm{C_i}$ not visible in the spectrum.

Elemental analysis calculated for $\mathrm{C_{29}H_{39}I_2P_3Pt}$ (M = 929.4342 g/mol): % C = 37.47%, % H = 4.23%, found % C = 38.01%, % H = 4.29%.

Synthesis of 2c. To a suspension of **2** (0.373 g, 0.376 mmol) in 4 mL of DME was dropwise added 1.32 mL of a solution of 1,6-dibromohexane (0.376 mmol, C_{M} = 0.284 M) at −30 °C. The reaction mixture was allowed to warm to room temperature, and NMR spectra were acquired. The reaction was complete (no signals of the starting complex) after 30 min. The solvent was evaporated, and the oily residue was partially dissolved in pentane. A small amount of yellow crystals of **2c** suitable for X-ray analysis were obtained upon dilution of the pentane solution at room temperature.

NMR data for **2c**:

^{1}H NMR ($\mathrm{C_6D_6}$, 400 MHz, 298 K δ): 0.94 (m, overlapped, 6H, $\mathrm{PCH_2}$ and $\mathrm{CH_2}$), 1.33 (m, overlapped, 4H, $\mathrm{CH_2}$), 1.42 (d, $^3J_{\mathrm{PH}}$ = 15 Hz, 9H, $\mathrm{C(CH_3)_3}$), 1.51 (d, $^3J_{\mathrm{PH}}$ = 16 Hz, 9H, $\mathrm{C(CH_3)_3}$), 1.78 (broad m, 2H, $\mathrm{BrCH_2}$), 1.90 (s, 9H, $p\text{-}\mathrm{CH_3}\text{−}\mathrm{C_6H_4}$), 6.94 (m, 6H, $\mathrm{C_{Ar}}$−$\mathrm{H_m}$), 7.86 (m, 6H, $\mathrm{C_{Ar}}$−$\mathrm{H_o}$).

$^{31}\mathrm{P}\{^1\mathrm{H}\}$ NMR ($\mathrm{C_6D_6}$, 162 MHz, 298 K, δ): 54.8 (dd, $^1J_{\mathrm{PP}}$ = 483 Hz, $^2J_{\mathrm{PP}}$ = 299 Hz, $^1J_{\mathrm{PPt}}$ = 1694 Hz, $t\mathrm{Bu_2P}$), 23.4 (dd, $^2J_{\mathrm{PP}}$ = 299 Hz, $^2J_{\mathrm{PP}}$ = 8 Hz, $^1J_{\mathrm{PPt}}$ = 3606 Hz, $p\mathrm{Tol_3P}$), −68.0 (dd, $^1J_{\mathrm{PP}}$ = 483 Hz $^2J_{\mathrm{PP}}$ = 8 Hz, $^1J_{\mathrm{PPt}}$ = 432 Hz, $\mathrm{P(CH_2)_6Br}$).

$^{13}\mathrm{C}\{^1\mathrm{H}\}$ NMR ($\mathrm{C_6D_6}$, 100 MHz, 298 K δ): 20.0 (dd, $^1J_{\mathrm{CP}}$ = 50 Hz, $^2J_{\mathrm{CP}}$ = 7 Hz, $\mathrm{PCH_2}$), 20.8 (s, $p\text{-}\mathrm{CH_3}\text{−}\mathrm{C_6H_4}$), 27.6 (s, $\mathrm{CH_2}$), 30.0 (m, $\mathrm{CH_2}$), 30.8 (m, $\mathrm{CH_2}$), 31.6 (broad d, $^2J_{\mathrm{CP}}$ = 8 Hz, $\mathrm{C(CH_3)_3}$), 32.2 (broad m, $\mathrm{C(CH_3)_3}$), 32.4 (s, $\mathrm{CH_2}$)), 33.2 (s, $\mathrm{CH_2}$), 36.1 (m, $\mathrm{C(CH_3)_3}$), 37.6 (m, $\mathrm{C(CH_3)_3}$), 128.9 (d, $^3J_{\mathrm{CP}}$ = 11 Hz, $\mathrm{C_m}$), 130.7 (d, $^1J_{\mathrm{CP}}$ = 50 Hz, $\mathrm{C_i}$), 134.6 (d, $^2J_{\mathrm{CP}}$ = 12 Hz, $\mathrm{C_o}$), 139.9 (broad s, $\mathrm{C_p}$).

Synthesis of 3. A slightly modified version of the synthesis of $[(\mathrm{dppe})\mathrm{Pt}(\eta^2\text{-}t\mathrm{Bu_2P{=}P})]$ previously described in the literature was used.[13] A solution of dppe in toluene was added to a suspension of **2** in toluene at room temperature, and the mixture was stirred for 2−3 days. The volume of the solution was decreased to a quarter of the original volume and it was stirred for another day. Then, the solution was layered with two volumes of petroleum ether, and the resulting precipitate was washed with a 1:2 toluene/ether mixture, resulting in pure $[(\mathrm{dppe})\mathrm{Pt}(\eta^2\text{-}t\mathrm{Bu_2P{=}P})]$ as a solid (~60% yield).

NMR data for **3**: see ref 13.

Synthesis of 3a. To a suspension of **3** (0.385 g, 0.5 mmol) in toluene was dropwise added 0.577 mL of a solution of methyl iodide

https://dx.doi.org/10.1021/acs.inorgchem.0c00091
Inorg. Chem. 2020, 59, 5463−5474

(0.5 mmol, C_M = 0.653 M) at −30 °C. The reaction mixture was then warmed to room temperature, and a large amount of white solid formed. The solvent was evaporated, and the solid residue was dissolved in THF. Colorless crystals of **3a** (290 mg, 0.295 mmol, 60% yield) were obtained from the THF solution at −20 °C.

NMR data for **3a**:

^{1}H NMR ($CDCl_3$, 400 MHz, 298 K δ): 0.99 (m, 3H, PC**H**$_3$), 1.11 (d, $^3J_{PH}$ = 16 Hz, 9H, C(C**H**$_3$)$_3$), 1.16 (d, $^3J_{PH}$ = 16 Hz, 9H, C(C**H**$_3$)$_3$), 1.18 (m, 4H, THF), 2.50 (broad m, 2H, C**H**$_2$, dppe), 2.87 (broad m, 2H, C**H**$_2$, dppe), 3.67 (m, 4H, THF), 7.31−7.56 (m, overlapped, 16 H, C_{Ar}-**H**), 7.66 (m, overlapped, 2H, C_{Ar}-**H**), 7.82 (m, overlapped, 2H, C_{Ar}-**H**).

^{31}P{^{1}H} NMR ($CDCl_3$, 162 MHz, 298 K, δ): 54.5 (ddd, $^1J_{PP}$ = 455 Hz, $^2J_{PP}$ = 230 Hz, $^2J_{PP}$ = 24 Hz, $^1J_{PPt}$ = 1710 Hz, *t*Bu$_2$**P**), 51.2 (dd, $^2J_{PP}$ = 230 Hz, $^2J_{PP}$ = 36 Hz, $^1J_{PPt}$ = 2990 Hz, dppe), 49.9 (dd, $^2J_{PP}$ = 71 Hz, $^2J_{PP}$ = 24 Hz, $^1J_{PPt}$ = 2774 Hz, dppe), −130.8 (ddd, $^1J_{PP}$ = 455 Hz, $^2J_{PP}$ = 71 Hz, $^2J_{PP}$ = 36 Hz, $^1J_{PPt}$ 290 Hz, **P**Me).

^{13}C{^{1}H} NMR ($CDCl_3$, 100 MHz, 298 K δ): 5.13 (dd, $^1J_{CP}$ = 52 Hz, $^2J_{CP}$ = 8 Hz, $^3J_{CP}$ = 4 Hz, P**C**H$_3$), 25.6 (s, THF), 28.3 (dd, $^2J_{CP}$ = 37 Hz, $^2J_{CP}$ = 13 Hz, **C**H$_2$, dppe), 30.6 (ddd, $^2J_{CP}$ = 37 Hz, $^2J_{CP}$ = 11 Hz, $^3J_{CP}$ = 4 Hz **C**H$_2$, dppe), 31.7 (d, $^2J_{CP}$ = 9 Hz, C(**C**H$_3$)$_3$), 31.8 (m, overlapped, C(**C**H$_3$)$_3$), 36.3 (broad m, **C**(CH$_3$)$_3$), 38.2 (broad m, **C**(CH$_3$)$_3$), 68.0 (s, THF), 129.2−134.2 (m, overlapped, **C**$_{Ar}$, dppe).

Elemental analysis calculated for $C_{39}H_{53}IOP_4Pt$ (M = 983.7210g/mol): % C = 47.62%, % H = 5.43%, found % C = 47.60%, % H = 5.54%.

Synthesis of 3b. To a suspension of **3** (0.385 g, 0.5 mmol) in 4 mL toluene was dropwise added a solution of 1,2-diiodoethane (0.141 g, 0.500 mmol) in 1 mL of toluene at −30 °C. The solvent was evaporated, and the solid residue was partially dissolved in toluene and the rest was dissolved in DCM. A small amount of orange solid (polyphosphorus compounds) was not soluble in any accessible solvent. After evaporation of the toluene, the oily residue of *t*Bu$_2$PI[48] remained, which was confirmed by NMR spectroscopy. Large yellow crystals of **3b**[42] were obtained from a DCM solution at −30 °C.

Synthesis of 3c. To a suspension of **3** (0.308 g, 0.400 mmol) in 4 mL of DME was dropwise added 0.847 mL of a solution of 1,2-dibromoethane (0.400 mmol, C_M = 0.472 M) at −30 °C. Then, the mixture was allowed to warm to room temperature, and a substantial amount of yellow residue formed during heating. The residue was washed with toluene and dissolved in DCM. The DCM solution was further layered with toluene, and large, light-green crystals of **3c** (0.111 g, 0.108 mmol, yield 27%) suitable for X-ray analysis were obtained at room temperature.

NMR data for **3c**:

^{1}H NMR ($CDCl_3$, 400 MHz, 298 K δ): 0.82 (broad d, overlapped, $^3J_{PH}$ = 16 Hz, 36H, C(C**H**$_3$)$_3$), 1.54 (broad s, 2H, C**H**$_2$, dppe), 2.12 (broad s, 2H, C**H**$_2$, dppe), 2.77 (broad s, 2H, C**H**$_2$, dppe), 3.16 (broad s, 2H, C**H**$_2$, dppe), 5.31 (s, 4H, C**H**$_2$Cl$_2$), 7.36 (broad, s, 4H, C_{Ar}−**H**), 7.52 (broad, s, 18H, C_{Ar}−**H**), 7.71 (broad, s, 14H, C_{Ar}−**H**), 8.14 (broad, s, 4H, C_{Ar}−**H**).

^{31}P{^{1}H} NMR ($CDCl_3$, 162 MHz, 298 K, δ): 67.9 (m, *t*Bu$_2$**P**), 50.1 (d, $^2J_{PP}$ = 120 Hz, dppe), 47.1 (m, dppe), −120.1 (m, **P**).

^{13}C{^{1}H} NMR ($CDCl_3$, 100 MHz, 298 K δ): 30.2 (m, **C**H$_2$, dppe), 30.6 (m, **C**H$_2$, dppe), 31.4 (broad s, C(**C**H$_3$)$_3$), 37.2 (very broad m, **C**(CH$_3$)$_3$), 40.4 (very broad m, **C**(CH$_3$)$_3$), 53.4 (s, **C**H$_2$Cl$_2$), 129.7 (broad s, **C**$_{Ar}$, dppe), 130.5 (broad m, overlapped, **C**$_{Ar}$, dppe), 131.5 (broad m, overlapped, **C**$_{Ar}$, dppe), 132.6 (broad m, overlapped, **C**$_{Ar}$, dppe), 133.4 (broad m, overlapped, **C**$_{Ar}$, dppe), 134.7 (broad m, overlapped, **C**$_{Ar}$, dppe).

Elemental analysis calculated for $C_{36}H_{46}BrCl_4P_4Pt$ (M = 1019.44 g/mol): % C = 42.41%, % H = 4.55%, found % C = 42.66%, % H = 4.60%.

■ ASSOCIATED CONTENT

Supporting Information

The Supporting Information is available free of charge at https://pubs.acs.org/doi/10.1021/acs.inorgchem.0c00091.

Crystallographic details, spectroscopic details, and computational details (PDF)

Accession Codes

CCDC 1963412−1963419 contain the supplementary crystallographic data for this paper. These data can be obtained free of charge via www.ccdc.cam.ac.uk/data_request/cif, or by emailing data_request@ccdc.cam.ac.uk, or by contacting The Cambridge Crystallographic Data Centre, 12 Union Road, Cambridge CB2 1EZ, UK; fax: +44 1223 336033.

■ AUTHOR INFORMATION

Corresponding Author

Rafał Grubba − *Department of Inorganic Chemistry, Faculty of Chemistry, Gdańsk University of Technology 80-233 Gdańsk, Poland*; orcid.org/0000-0001-6965-2304; Email: rafal.grubba@pg.edu.pl

Authors

Anna Ordyszewska − *Department of Inorganic Chemistry, Faculty of Chemistry, Gdańsk University of Technology 80-233 Gdańsk, Poland*

Natalia Szynkiewicz − *Department of Inorganic Chemistry, Faculty of Chemistry, Gdańsk University of Technology 80-233 Gdańsk, Poland*

Jarosław Chojnacki − *Department of Inorganic Chemistry, Faculty of Chemistry, Gdańsk University of Technology 80-233 Gdańsk, Poland*

Jerzy Pikies − *Department of Inorganic Chemistry, Faculty of Chemistry, Gdańsk University of Technology 80-233 Gdańsk, Poland*

Complete contact information is available at: https://pubs.acs.org/10.1021/acs.inorgchem.0c00091

Notes

The authors declare no competing financial interest.

■ ACKNOWLEDGMENTS

A.O. and J.P. thank the National Science Centre, Poland (Grant 2017/25/N/ST5/00766) for financial support. The authors thank the TASK Computational Center for access to computational resources.

■ REFERENCES

(1) Waterman, R. Metal-Phosphido and -Phosphinidene Complexes in P-E Bond-Forming Reactions. *Dalton Trans.* **2009**, *9226* (1), 18−26.

(2) Mathey, F. The Development of a Carbene-like Chemistry with Terminal Phosphinidene Complexes. *Angew. Chem., Int. Ed. Engl.* **1987**, *26* (4), 275−286.

(3) Mathey, F.; Huy, N. H. T.; Marinetti, A. Electrophilic Terminal-Phosphinidene Complexes: Versatile Phosphorus Analogues of Singlet Carbenes. *Helv. Chim. Acta* **2001**, *84* (10), 2938−2957.

(4) Lammertsma, K. Phosphinidenes. *Top. Curr. Chem.* **2003**, *229*, 95−119.

(5) Mathey, F. Developing the Chemistry of Monovalent Phosphorus. *Dalton Trans.* **2007**, *2007* (19), 1861−1868.

(6) Cowley, A. H. Terminal Phosphinidene and Heavier Congeneric Complexes. The Quest Is Over. *Acc. Chem. Res.* **1997**, *30* (11), 445−451.

(7) Sánchez-Nieves, J.; Sterenberg, B. T.; Udachin, K. A.; Carty, A. J. A Thermally Stable and Sterically Unprotected Terminal Electrophilic Phosphinidene Complex of Cobalt and Its Conversion to an H1-Phosphirene. *J. Am. Chem. Soc.* **2003**, *125* (9), 2404−2405.

(8) Graham, T. W.; Udachin, K. A.; Zgierski, M. Z.; Carty, A. J. Synthesis and Structural Characterization of the First Thermally Stable, Neutral, and Electrophilic Phosphinidene Complexes of Vanadium. *Organometallics* **2011**, *30* (6), 1382−1388.
(9) Aktas, H.; Slootweg, J. C.; Lammertsma, K. Nucleophilic Phosphinidene Complexes: Access and Applicability. *Angew. Chem., Int. Ed.* **2010**, *49* (12), 2102−2113.
(10) Ehlers, A. W.; Baerends, E. J.; Lammertsma, K. Nucleophilic or Electrophilic Phosphinidene Complexes ML_n=PH; What Makes the Difference? *J. Am. Chem. Soc.* **2002**, *124* (11), 2831−2838.
(11) Grubba, R.; Baranowska, K.; Chojnacki, J.; Pikies, J. Access to Side-On Bonded Tungsten Phosphanylphosphinidene Complexes. *Eur. J. Inorg. Chem.* **2012**, *2012* (20), 3263−3265.
(12) Domańska-Babul, W.; Chojnacki, J.; Matern, E.; Pikies, J. Reactions of R_2P-P($SiMe_3$)Li with $[(R'_3P)_2PtCl_2]$. A general and efficient entry to phosphanylphosphinidene complexes of platinum. Syntheses and structures of $[(\eta^2$-P═P*i*$Pr_2)Pt(p$-$Tol_3P)_2]$, $[(\eta^2$-P═P*t*$Bu_2)Pt(p$-$Tol_3P)_2]$, $[\{\eta^2$-P═P(N*i*$Pr_2)_2\}Pt(p$-$Tol_3P)_2]$ and $[\{(Et_2PhP)_2Pt\}_2P_2]$. *Dalton Trans.* **2009**, *668504* (1), 146−151.
(13) Krautscheid, H.; Matern, E.; Fritz, G.; Pikies, J. Komplexchemie P-reicher Phosphane und Silylphosphane. XIV. Einfluß der Chelatbildner dppe und dppp auf die Bildung und die Eigenschaften der Pt-Komplexe des *t*Bu_2P-P. *Z. Anorg. Allg. Chem.* **1998**, *624*, 501−505.
(14) Figueroa, J. S.; Cummins, C. C. Diorganophosphanylphosphinidenes as Complexed Ligands: Synthesis via an Anionic Terminal Phosphide of Niobium. *Angew. Chem., Int. Ed.* **2004**, *43* (8), 984−988.
(15) Fox, A. R.; Clough, C. R.; Piro, N. A.; Cummins, C. C. A Terminal Nitride-to-Phosphide Conversion Sequence Followed by Tungsten Phosphide Functionalization Using a Diphenylphosphenium Synthon. *Angew. Chem., Int. Ed.* **2007**, *46* (6), 973−976.
(16) Hansmann, M. M.; Jazzar, R.; Bertrand, G. Singlet (Phosphino)Phosphinidenes Are Electrophilic. *J. Am. Chem. Soc.* **2016**, *138* (27), 8356−8359.
(17) Olkowska-Oetzel, J.; Pikies, J. Chemistry of the Phosphinophosphinidene *t*Bu_2P-P, a Novel π-Electron Ligand. *Appl. Organomet. Chem.* **2003**, *17* (1), 28−35.
(18) Zauliczny, M.; Ordyszewska, A.; Pikies, J.; Grubba, R. Bonding in Phosphanylphosphinidene Complexes of Transition Metals and Their Correlation with Structures, ^{31}P NMR Spectra, and Reactivities. *Eur. J. Inorg. Chem.* **2018**, *2018*, 3131.
(19) Cummins, C. C.; Schrock, R. R.; Davis, W. M. Phosphinidenetantalum(V) Complexes of the Type [(N_3N)Ta = PR] as Phospha-Wittig Reagents (R = Ph, Cy, *t*Bu, N_3N = $Me_3SiNCCH_2CH_2)_3N$). *Angew. Chem., Int. Ed. Engl.* **1993**, *32* (5), 756−759.
(20) Wicker, B. F.; Scott, J.; Andino, J. G.; Gao, X.; Park, H.; Pink, M.; Mindiola, D. J. Phosphinidene Complexes of Scandium: Powerful PAr Group-Transfer Vehicles to Organic and Inorganic Substrates. *J. Am. Chem. Soc.* **2010**, *132* (11), 3691−3693.
(21) Hou, Z.; Breen, T. L.; Stephan, D. W. Formation and Reactivity of the Early Metal Phosphides and Phosphinidenes Cp^*_2Zr:PR, $Cp^*_2Zr(PR)_2$, and $Cp^*_2Zr(PR)_3$. *Organometallics* **1993**, *12* (8), 3158−3167.
(22) Urnezius, E.; Lam, K. C.; Rheingold, A. L.; Protasiewicz, J. D. Triphosphane Formation from the Terminal Zirconium Phosphinidene Complex [Cp_2Zr = PDmp(PMe_3)] (Dmp = 2,6-$Mes_2C_6H_3$) and Crystal Structure of DmpP($PPh_2)_2$. *J. Organomet. Chem.* **2001**, *630* (2), 193−197.
(23) Breen, T. L.; Stephan, D. W. Phosphinidene Transfer Reactions of the Terminal Phosphinidene Complex Cp_2Zr(:PC_6H_2-2,4,6-*t*-Bu_3)(PMe_3). *J. Am. Chem. Soc.* **1995**, *117* (48), 11914−11921.
(24) Ziółkowska, A.; Szynkiewicz, N.; Ponikiewski, Ł. Molecular Structures of the Phospha-Wittig Reaction Intermediate: Initial Step in the Synthesis of Compounds with a C = P-P Bond as Products in the Phospha-Wittig Reaction. *Organometallics* **2019**, *38*, 2873−2877.
(25) Alvarez, C. M.; Alvarez, M. A.; García, M. E.; González, R.; Ruiz, M. A.; Hamidov, H.; Jeffery, J. C. High-Yield Synthesis and Reactivity of Stable Diiron Complexes with Bent-Phosphinidene Bridges. *Organometallics* **2005**, *24* (23), 5503−5505.
(26) Alvarez, M. A.; García, M. E.; González, R.; Ruiz, M. a. Reactions of the Phosphinidene-Bridged Complexes [$Fe_2(\eta^5$-$C_5H_5)_2(\mu$-PR)(μ-CO)$(CO)_2$] (R = Cy, Ph) with Electrophiles Based on p-Block Elements. *Dalton Trans.* **2012**, *41* (48), 14498.
(27) Termaten, A. T.; Nijbacker, T.; Schakel, M.; Lutz, M.; Spek, A. L.; Lammertsma, K. Synthesis of Novel Terminal Iridium Phosphinidene Complexes. *Organometallics* **2002**, *21* (15), 3196−3202.
(28) Kourkine, I.; Glueck, D. Synthesis and Reactivity of a Dimeric Platinum Phosphinidene Complex. *Inorg. Chem.* **1997**, *36* (9), 5160−5164.
(29) Arduengo, A. J.; Calabrese, J. C.; Cowley, A. H.; Dias, H. V. R.; Goerlich, J. R.; Marshall, W. J.; Riegel, B. Carbene-Pnictinidene Adducts. *Inorg. Chem.* **1997**, *36* (10), 2151−2158.
(30) Back, O.; Henry-Ellinger, M.; Martin, C. D.; Martin, D.; Bertrand, G. ^{31}P NMR Chemical Shifts of Carbene-Phosphinidene Adducts as an Indicator of the π-Accepting Properties of Carbenes. *Angew. Chem., Int. Ed.* **2013**, *52* (10), 2939−2943.
(31) Roy, S.; Mondal, K. C.; Kundu, S.; Li, B.; Schürmann, C. J.; Dutta, S.; Koley, D.; Herbst-Irmer, R.; Stalke, D.; Roesky, H. W. Two Structurally Characterized Conformational Isomers with Different C-P Bonds. *Chem. - Eur. J.* **2017**, *23* (50), 12153−12157.
(32) Kundu, S.; Sinhababu, S.; Siddiqui, M. M.; Luebben, A. V.; Dittrich, B.; Yang, T.; Frenking, G.; Roesky, H. W. Comparison of Two Phosphinidenes Binding to Silicon(IV)Dichloride as Well as to Silylene. *J. Am. Chem. Soc.* **2018**, *140* (30), 9409−9412.
(33) Pikies, J.; Baum, E.; Matern, E.; Chojnacki, J.; Grubba, R.; Robaszkiewicz, A. A New Synthetic Entry to Phosphinophosphinidene Complexes. Synthesis and Structural Characterisation of the First Side-on Bonded and the First Terminally Bonded Phosphinophosphinidene Zirconium Complexes. *Chem. Commun.* **2004**, *98* (21), 2478−2479.
(34) Grubba, R.; Ordyszewska, A.; Kaniewska, K.; Ponikiewski, Ł.; Chojnacki, J.; Gudat, D.; Pikies, J. Reactivity of Phosphanylphosphinidene Complex of Tungsten(VI) toward Phosphines: A New Method of Synthesis of Catena-Polyphosphorus Ligands. *Inorg. Chem.* **2015**, *54* (17), 8380−8387.
(35) Grubba, R.; Ordyszewska, A.; Ponikiewski, Ł.; Gudat, D.; Pikies, J. An Investigation on the Chemistry of the R_2P = P Ligand: Reactions of a Phosphanylphosphinidene Complex of Tungsten(VI) with Electrophilic Reagents. *Dalton Trans.* **2016**, *45* (5), 2172−2179.
(36) Ponikiewski, Ł.; Ziółkowska, A.; Pikies, J. Reactions of Lithiated Diphosphanes R_2P-P($SiMe_3$)Li (R = *t*Bu and *i*Pr) with [^{Me}NacnacTiCl_2·THF] and [^{Me}NacnacTiCl_3]. Formation and Structure of Titanium^{III} and Titanium^{IV} β-Diketiminato Complexes Bearing the Side-on Phosphanylphosphido and Phosphanylphosphinidene Functionalities. *Inorg. Chem.* **2017**, *56* (3), 1094−1103.
(37) Krautscheid, H.; Matern, E.; Kovacs, I.; Fritz, G.; Pikies, J. Komplexchemie P-reicher Phosphane und Silylphosphane. XIV. Phosphinophosphiniden *t*Bu_2P-P als Ligand in den Pt-Komplexen $[\{\eta^2$-*t*Bu_2P-P$\}$Pt($PPh_3)_2]$ und $[\{\eta^2$-*t*Bu_2P-P$\}$Pt($PEtPh_2)_2]$. *Z. Anorg. Allg. Chem.* **1997**, *623*, 1917−1924.
(38) Wright, W. R. H.; Batsanov, A. S.; Howard, J. A. K.; Tooze, R. P.; Hanton, M. J.; Dyer, P. W. Exploring the Reactivity of Tungsten Bis(Imido) Dimethyl Complexes with Methyl Aluminium Reagents: Implications for Ethylene Dimerization. *Dalton Trans.* **2010**, *39* (30), 7038−7045.
(39) Pyykkö, P.; Atsumi, M. Molecular Single-Bond Covalent Radii for Elements 1−118. *Chem. - Eur. J.* **2009**, *15* (1), 186−197.
(40) Schmiedeskamp, B. K.; Reising, J. G.; Malisch, W.; Hindahl, K.; Schemm, R.; Sheldrick, W. S. Phosphenium Transition Metal Complexes. Part 34. P-Functionalized Cyclic Phosphinidenemetallophosphoranes [Cyclic] $Cp(CO)_2$W-P(X)(t-Bu)-P(t-Bu) (X = Cl, H): Direct Formation from Metallophosphines and Transformation Reactions. *Organometallics* **1995**, *14* (10), 4446−4448.
(41) Weber, L.; Noveski, G.; Stammler, H.-G.; Neumann, B. Über Den Phosphandiyl-Transfer von Invers-Polarisierten Phosphaalkenen

https://dx.doi.org/10.1021/acs.inorgchem.0c00091
Inorg. Chem. 2020, 59, 5463−5474

$R_1P = C(NMe_2)_2$ (R_1 = tBu, Cy, Ph, H) Auf Phospheniumkomplexe $[(\eta^5\text{-}C_5H_5)(CO)_2M = P(R_2)R_3]$ ($R_2 = R_3$ = Ph; R_2 = tBu, R_3 = H; R_2 = Ph, $R_3 = N(SiMe_3)_2$). *Z. Anorg. Allg. Chem.* **2007**, *633* (7), 994−999.

(42) Sivaramakrishna, A.; Su, H.; Moss, J. R. [1,2-Bis-(Diphenylphosphino)Ethane]Diiodidoplatinum(II) Dichloromethane Disolvate. *Acta Crystallogr., Sect. E: Struct. Rep. Online* **2007**, *63* (11), No. m2648.

(43) Matern, E.; Pikies, J.; Fritz, G. Zum Einfluß Der PR_3-Liganden Auf Bildung Und Eigenschaften Der Phosphinophosphiniden-Komplexe $[\{\eta^2\text{-}t\text{Bu}_2\text{P-P}\}\text{Pt}(PR_3)_2]$ Und $[\{\eta^2\text{-}t\text{Bu}_2\text{P1-P2}\}\text{Pt}(\text{P3R}_3)\text{-}(\text{P4R}'_3)]$. *Z. Anorg. Allg. Chem.* **2000**, *626* (10), 2136−2142.

(44) Chatt, J.; Mason, R.; Meek, D. W. Unusually Large Platinum-Phosphorus Coupling Constants in Platinum(0) Tetraphosphine Complexes. *J. Am. Chem. Soc.* **1975**, *97* (13), 3826−3827.

(45) Melník, M.; Mikuš, P. Organophosphines in Organoplatinum Complexes - Structural Aspects of *Trans*-PtP_2CCl Derivatives. *J. Organomet. Chem.* **2016**, *819*, 46−52.

(46) Grubba, R.; Zauliczny, M.; Ponikiewski, Ł.; Pikies, J. The Reactivity of 1,1-Dichloro-2,2-Di-Tert-Butyldiphosphane towards Lithiated Metal Carbonyls: A New Entry to Phosphanylphosphinidene Dimers. *Dalton Trans.* **2016**, *45* (12), 4961.

(47) Loss, S.; Widauer, C.; Grützmacher, H. Strong P = P π Bonds: The First Synthesis of a Stable Phosphanyl Phosphenium Ion. *Angew. Chem., Int. Ed.* **1999**, *38* (22), 3329−3331.

(48) Kovacs, I.; Fritz, G. $t\text{Bu}_2\text{P-P} = \text{P(X)}t\text{Bu}_2$-Ylide (X = C1, Br, I) Durch Halogenierung von $[t\text{Bu}_2\text{P}]_2\text{P-SiMe}_3$. *Z. Anorg. Allg. Chem.* **1994**, *620*, 1364−1366.

https://dx.doi.org/10.1021/acs.inorgchem.0c00091
Inorg. Chem. 2020, 59, 5463−5474